Aalto-yliopisto
Insinööritieteiden
korkeakoulu

Mika Miettinen

Vibration Management of Floating Floor Structures in Ships

Thesis submitted for examination for the degree of Master of Science in Technology

Espoo 29.7.2019
Thesis supervisor: Luc St-Pierre, Assistant Professor
Thesis advisor: Jonas Packalén, M.Sc. (Tech)

Aalto University
School of Engineering

Aalto University, P.O. BOX 11000, 00076 AALTO
www.aalto.fi

Abstract of master's thesis

Author Mika Miettinen

Title of thesis Vibration Management of Floating Floor Structures in Ships

Master programme Mechanical Engineering **Code** ENG25

Thesis supervisor Luc St-Pierre, Assistant Professor

Thesis advisor(s) Jonas Packalén, M.Sc. (Tech)

Date 29.7.2019 **Number of pages** 62 **Language** English

Abstract

Floating floors, visco-elastic floors and combination floors are often used to reduce noise and vibration levels e.g. in ship cabins. However, in a few cases at Arctech Helsinki Shipyard, floating floors have been detected to amplify vibrations in ship cabins. The goal of this thesis was to enhance modelling methods to take the vibrations of floating floors better into account in a design process.

Two different cases were used as references, Icebreaking Supply Vessels NB506 and NB511. In both cases excessive vibrations were detected during the seatrials. In NB506 excessive vibrations occurred in the wheelhouse of the ship and in NB511 in the accommodation area.

A few different approaches were briefly investigated, a simple mathematical model based on the basic concepts of vibration dynamics, a modelling method based on the finite element method and an analysis based on experimental modal analysis. The method based on finite element analysis was selected for further development since FE-analysis was already utilized in the design process.

The floating floor structure was modelled by using shell and solid elements. Steel decks and top plates were modelled as shell elements and mineral wool layer as solid elements. The used material model for mineral wool was based on the behavior of wool under static loading. The material model was verified by comparing FE-model's dynamic response with the results of dynamic stiffness definition and actual measurement data.

In the case study, the FE-model of NB511 was utilized. The developed submodelling technique was used to solve the response of the local structure of 2nd Bridge Deck with implemented floating floor structure. Results of the analysis were quite auspicious when the critical area localization was considered. The results showed that the higher vibration levels can be distinguished at the locations where vibration problems occurred during the seatrials, when compared with vibration levels of other cabins in the 2nd Bridge Deck. However, comparison between FE-model response and more detailed measurements of real structures would be needed for the complete verification of the modelling method.

Keywords soundproofing floor, floating floor, vibration analysis, shipbuilding

Aalto-yliopisto
Insinööritieteiden
korkeakoulu

Aalto-yliopisto, PL 11000, 00076 AALTO
www.aalto.fi

Diplomityön tiivistelmä

Tekijä Mika Miettinen		
Työn nimi Uivien lattioiden värähtelyjen hallinta laivoissa		
Maisteriohjelma Konetekniikka		**Koodi** ENG25
Työn valvoja Luc St-Pierre, Apulaisprofessori		
Työn ohjaaja(t) Jonas Packalén, DI		
Päivämäärä 29.07.2019	**Sivumäärä** 62	**Kieli** englanti

Tiivistelmä

Uivia lattioita, viskoelastisia lattioita sekä yhdistelmälattioita käytetään usein vähentämään melua sekä värähtelyjä esimeriksi laivojen hyteissä. Arctech Helsinki Shipyardin telakalla on havaittu muutamissa tapauksissa, että uivat lattiat saattavat vahvistavaa hyttien lattioiden värähtelyjä joissakin tilanteissa. Tämän diplomityön tavoitteena on kehittää mallinnusmenetelmiä ottamaan paremmin huomioon uivien lattioiden värähtelykäyttäytyminen laivan suunnitteluprosessissa.

Tässä diplomistyössä käytettiin referenssinä kahta eri jäätä murtavaa huoltoalusta, NB506:ta ja NB511:tä. Molemmissa tapauksissa merikokeiden aikana laivoissa havaittiin huomattavia värähtelyjä. NB506:n tapauksessa värähtelyt ilmenivät laivan komentosillalla ja NB511:n tapauksessa laivan majoitustiloissa.

Muutamia eri lähestymistapoja tutkittiin lyhyesti. Yksinkertainen matemaattinen malli, joka perustuu värähtelymekaniikan peruskäsitteisiin; mallinnusmenetelmä, joka perustuu äärelliseen elementtimenetelmään, sekä kokeelliseen moodianalyysiin perustuva menetelmä. Elementtimenetelmään perustuva menetelmä valittiin jatkokehitykseen, sillä elementtimenetelmää hyödynnetään jo valmiiksi laivojen suunnitteluprosessissa.

Uiva lattia mallinnettiin käyttämällä kuori- sekä tilavuuselementtejä. Laivan teräskannet sekä päällyslevyt mallinnettiin kuorielementeillä ja villakerros tilavuuselementeillä. Käytetty materiaalimalli perustui mineraalivillan käyttäytymiseen staattisen kuormituksen alla. Materiaalimalli vahvistettiin vertaamalla elementtimallista saatua vastetta dynaamisen jäykkyyden määritelmään sekä olemassa olevaan mittausdataan.

Työn soveltavassa osassa hyödynnettiin NB511-laivan elementtimallia. Diplomityössä kehitettyä alimallinnusmenetelmää hyödynnettiin majoitustilojen paikallisen mallin ratkaisussa. Majoitustiloihin oli paikallisessa mallissa mallinnettu uiva lattiarakenne. Värähtelyanalyysistä saadut tulokset olivat melko lupaavia mitä tulee kriittisten alueiden paikallistamiseen. Hytit, joissa havaittiin merikokeilla korkeampia värähtelytasoja, erottuivat myös äärelliseen elementtimenetelmään perustuvan värähtelyanalyysin tulosten perusteella hyteistä, joissa ongelmia ei havaittu. Lopullisen mallinnusmenetelmän vahvistaminen vaatisi kuitenkin lisää vertailua numeerisen mallin sekä todellisesta rakenteesta saatujen mittaustulosten välillä.

Avainsanat ääntä eristävä lattiarakenne, uiva lattia, värähtelyanalyysi, laivanrakennus

Preface

Comfort on ships is an important topic in the shipbuilding industry. It is especially important in cruise ships and passenger ships. However, there is also an increasing need to improve comfort onboard in ships like icebreakers and other types of industrial ships. One way to manage noise and vibration problems in ships is to use soundproofing floor structures. However, sometimes these structures can generate unexpected vibration problems when excited by the machinery or propulsion system. The purpose of this thesis was to improve the design process to take better into account the dynamic behavior of floating floors. This thesis was written during the employment to Arctech Helsinki Shipyard.

I would like to thank my advisor Jonas Packalén from the shipyard and the supervising Professor Luc St-Pierre from Aalto University. Both provided me very valuable feedback and guidance during my thesis project. I would like to thank Janne Rantanen from the shipyard for his support and comments on the thesis project. Carsten "Brutus" Jorgensen from Sika group provided some great material and comments on my thesis topic, thank you. Also, I would like to thank all the colleagues I worked with at the shipyard as well as all the other people who contributed the project somehow.

I want to thank my awesome family, Hanna and Hertta, for their support during this project. Finally, I want to thank all my friends and family, especially my dad for his comments and feedback throughout the whole process.

Espoo 29.7.2019

Mika Miettinen

Table of Contents

Abstract
Tiivistelmä
Preface
1 Introduction 1
2 Background 3
3 Ship Vibrations 5
3.1 Global Vibrations 5
3.2 Local Vibrations 6
3.3 Vibration Sources 7
3.3.1 Propeller Excitation 7
3.3.2 Engine Excitation 8
3.3.3 Other Sources of Vibration 10
4 Vibrations Analysis of Ships Using Finite Element Analysis 12
4.1 Finite Element Model of a Ship 13
4.2 Finite Element Analysis Types 13
4.2.1 Normal Modes Analysis 13
4.2.2 Forced Response Analysis 14
5 Soundproofing Floor Structures 16
5.1 Floating Floors 16
5.2 Visco-Elastic Floors 19
5.3 Combination Floors 22
5.4 Dynamic Stiffness of Resilient Material in Floating Floors 25
5.5 Floor Structure Under Investigation 26
6 Preliminary Study of Modelling Methods 28
6.1 Simple Mathematical Model 28
6.2 Finite Element Modelling Approaches 28
6.3 Modal Analysis 29
7 Selected Approach – Finite Element Model 31
7.1 FE-model of the Floating Floor 31
7.2 Validation of the Material Model 31
7.2.1 Comparison of Natural Frequencies 32
7.2.2 Modelling of Dynamic Stiffness Measurements 34
7.3 Submodelling Procedure 38
8 Case Study – Vibration Analysis of a Ship 43
8.1 Finite Element Model of the Ship 43
8.2 Vibration Analysis of the Global Model 44
8.3 Submodel of Local Structure 47
8.4 Investigation of Floating Floor Model 48
8.4.1 Finite Element Model 48
8.4.2 Results of the Analysis 51
8.4.3 Interpretation of Results 57
9 Conclusions and Future Studies 59
References 61

1 Introduction

In the shipbuilding applications floating floors, visco-elastic floors and combination floors are used to reduce noise and vibration levels especially in the ship cabins at the critical locations. These structures are commonly used for instance above engine rooms and other areas with high intensity noise and vibration sources.

Although a good performance in noise reduction and improvement of the comfort in ship cabins is achieved in general, these soundproofing floor structures have been observed to generate unexpected mechanical vibrations. At the Arctech Helsinki Shipyard there have been multiple cases where considerable amount of vibrations has been detected in areas where soundproofing floor structures were installed. These events have occurred in cabins located in the accommodation area, as well as in the wheelhouse of a ship. In these cases, it seems that the floating floor structure amplifies the vibration of the decking plate to make the situation worse compared to the situation without the floating floor regard to comfort inside a ship cabin.

The goal of this thesis is to improve modelling methods to take vibrations of floating floors better into account in a design process. Because noise reduction is the main goal of using floating floor structures, vibrations at the frequencies below 50 Hz are not so well considered in the design phase. Usually, vibrations that exceed the limit values are discovered quite late, after the main design phase, in the testing phase. This project should produce some tools and methods to predict critical areas on early stages using vibration analysis tools, such as Finite Element Analysis. The scope of this thesis from the modelling point of view is limited to floating floors since including also the visco-elastic structures would diversify the scope of the thesis significantly.

The thesis is outlined as follows. Firstly, two cases are introduced where vibration problems were associated with floating floor structures. These were ships NB 506 and NB 511 build at the Arctech Helsinki Shipyard. The background chapter presents briefly ship types and what kind of vibration problems occurred in these ships, as well as used solutions to fix these problems. Secondly, the topic of ship vibrations is studied and summarized in the Ship Vibrations chapter. The Ship Vibrations chapter introduces the general concepts of vibration mechanics in shipbuilding applications. Also, the most common sources of vibrations are introduced in this chapter, such as excitations induced by the propulsion systems and engines of ships.

After introducing the concepts of ship vibrations, the general approaches of vibration analysis methods by using the means of Finite Element Analysis are presented. The Chapter 4 covers the general overview of the vibration analysis approaches based on the guidelines of different classification societies. The basic constructions and operating principles of different types of soundproofing floor structures are presented in Chapter 5. Also, the soundproofing capabilities of different types of floor structures are investigated.

In the preliminary studies a few different approaches are considered before the final decision about the modelling method is made. The preliminary study chapter introduces an idea of a simple mathematical model as well as a vibration analysis approach by using the means of the modal analysis in addition to the used approach based on the finite element analysis. The selected modelling approach that is based on the finite element analysis is introduced in Chapter 7. The chapter presents the procedure of material

property definition for the finite element model as well as the validation of the chosen material properties. Also, the used submodelling technique is presented and its performance is investigated in this chapter.

Next, the performance of the modelling method is studied by applying the developed model of the floating floor to the model of the NB 511 icebreaker. The created subodelling technique is used in the analysis. Different excitation cases as well as different load distributions on the top of the floating floor are analyzed.

In the final chapter, the study outcome will be concluded. The performance of used modelling methods will be discussed and possible solutions to vibration problems will be suggested. Finally, for further elaboration a few notions are highlighted for future studies and enhancing the utilized modelling methods.

2 Background

In the past, at the Arctech Helsinki Shipyard there have been multiple cases where considerable amount of vibrations has been detected in the areas with floating floor structures. In general, unwanted vibrations are not uncommon phenomenon in shipbuilding, however, two different cases have raised interests for more thorough investigations of the problem. Even though, this thesis studies the phenomena of the vibrations of marine floating floor structures in general, these two cases are used as a basis of the study.

The first case is NB 506 (Vitus Bering), Ice Breaking Support Vessel delivered in December 2012. It is a Multifunctional Icebreaking Supply Vessel (MIBSV) designed to be capable for all-year operations in the harsh conditions of the oil and gas fields near Sakhalin Island in Far East Russia. The length of the vessel is 100 meters and the breadth 21.7 meters, and it is capable to operate in 1.7 meter thick ice. The ship is powered by four diesel generators providing in total 18 MW of power and the propulsion is provided by two azimuthing podded type rudder propeller units with the propulsion power of 13 MW. [1]

During the first sea trial of NB 506 excessive vibrations of ceiling panels, the floor and equipment in the aft control position of the wheelhouse were detected while running bow thrusters at high power settings. After the sensory detection of heavy vibrations some measurements were arranged to determine the actual level of vibrations. Vibration peaks of 18 to 37 mm/s (RMS) were measured from the foundation of control consoles at the bow thrusters blade frequency when 100% power was applied. For instance, ISO 20283-5 gives a guideline value of 5 mm/s for vibration levels at the navigation bridge. [2]

To reduce the vibrations in the wheelhouse, external structural members were installed to strengthen the aft wheelhouse structure. Also, the equipment located on the top of floating floor were directly attached to the deck by using steel profiles. After these changes in the design, vibration levels decreased significantly to the 3 to 11 mm/s at the blade frequency.

The second one is NB 511, an icebreaking supply vessel that is an improved version of NB 506 (and its sister ship NB 507) and it is also designed to operate in the Sakhalin area. The ship was delivered in 2017. Main specifications are very similar to NB 506, however, there are some apparent changes, such as increase in the generated total power to 21 MW by using six diesel generators. The ship is also equipped with a moon pool to be able to operate as a diving support vessel in under water operations. [3]

As well as in the case of NB 506, during the first sea trial the vibration levels that exceeded the limit values were detected. The highest vibrations levels over 5 mm/s were measured in the cabin 71-019 exceeding the desired limit values. The limit value of these measurements is not clearly stated in the reporting. However, the measured value is high enough to exceed the guideline maximum value of 3.5 mm/s stated in ISO 20283-5. [2] Also, two other cabins did not meet the allowed vibration level criterion.

After the sea trial, vibration levels were measured while the structure was excited by a hydraulic shaker mounted on the top of the ship's bridge. A minute-long continuous sine sweep 10 to 20 Hz was used as an excitation. Vibrations were measured from the cabin 071-003 on the starboard side and from the cabin 071-019 on the port side of the ship. On

the starboard side the velocity peak above 1.0 mm/s (RMS) appeared at the frequency of 16 Hz and on the port side at the frequency of 15 Hz vibration velocities above 1.3 mm/s (RMS) occurred.

The vibration control was carried out by installing prototypes of tuned mass dampers on the cabin floors. Installing the dampers reduced vibrations on the starboard side to 0.4 mm/s (RMS) and on the port side below 0.4 mm/s (RMS). It should be noted that measurements were not done during the sea trial in normal operation conditions, thus these values can be used only to evaluate the amount of damping provided by mass dampeners.

Due to the promising results in the shaker test, three dampers were manufactured and installed into all three cabins with vibration issues. Dampers were tuned and tested during the second sea trial to achieve acceptable vibration levels at the 85 % propulsion power settings. The vibrations peak occurred at the blade excitation frequency close to 14 Hz at the 85 % propulsion power. By fine tuning the dampeners, acceptable vibration levels were achieved in all three cabins.

3 Ship Vibrations

Due to the increasing ship sizes and operating speeds as well as stricter levels of acceptable level of vibrations onboard, the topic of ship vibrations has become more important part of the design process of ships. Also, reducing weight of the ships quite often means lower stiffness that leads to decreasing natural frequencies of the system. [4] [5]

According to ISO 20283-5 the frequency range from 1 to 80 Hz is covered when vibrations of ships are considered [2]. At the higher end of the frequency range structure-borne noise is the dominant phenomena, while at the lower end of the frequency range is where for example the natural frequencies of global hull structures are located. Natural frequencies of local structures such as deck-panel structures, masts and deckhouse structures are often located at the somewhere at the middle of the frequency range [4]. To avoid problematic vibration behavior the structures should not be designed to have natural frequencies close to exciting frequencies such as engine and propeller excitation frequencies. However, because of the variations in these excitations, complete avoidance of resonance is usually inevitable. Also, the loading conditions of the ship might change the natural frequencies on local level, making the avoidance of the resonant frequencies even more difficult [4].

Four fundamental factors can be recognized that affects ship vibrations as well as vibrations problems in general. These are the applied excitation to the system, stiffness of the system, damping and the frequency ratio. Basically, all of these can be altered to achieve reduction in vibrations of the system. These actions can be for example, reduction in exciting force amplitude, increasing the stiffness of the system that is typical way to avoid resonant conditions i.e. where frequency ratio is close to unity. The fourth factor, the damping is usually small in ship structures, thus it does not influence vibration amplitude except close to resonant frequencies. Also, affecting the damping by the means of design is quite difficult, therefore it is not usually considered useful way to reduce vibrations of ships. While all of these four fundamental factors, excitation, stiffness, frequency ratio and damping are needed when ships vibrational response will be evaluated for example by the means of Finite Element Analysis, adequate effect on the vibration levels can be achieved already in the concept design face usually by concentrating on two of these, minimizing vibration excitations and avoiding excitation frequencies in the natural frequencies of major structures. [5]

3.1 Global Vibrations

The global response of the ship hull vibrates in five different modes, vertical and horizontal bending mode, torsional mode, longitudinal mode and coupled horizontal and torsional mode that exists especially in containerships. Under dynamic loading, the hull structure vibrates like a beam with both ends free (free-free) and it can respond in resonant or non-resonant manner. In Figure 1 first two vertical vibration modes of the ship are presented and a coupled horizontal-torsional mode is presented in Figure 2.

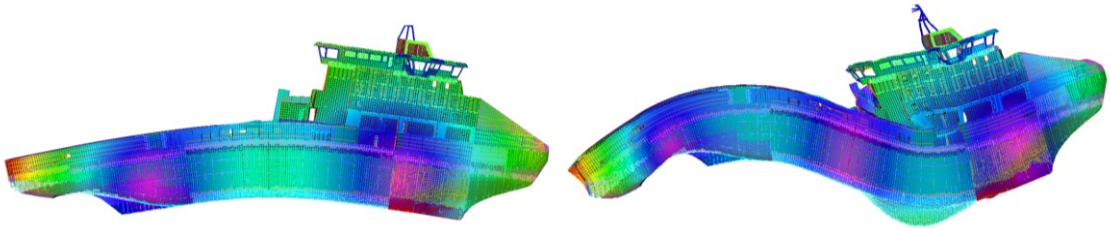

Figure 1. First two vertical modes of a ship

Usually ships have higher stiffness in the horizontal direction than vertical direction, thus typically lowest natural modes and frequencies appear in the vertical direction. However, sometimes torsional stiffness of the ship's hull might be low enough to lead the situation where lowest natural mode of the ship's hull is a torsional mode. Global modes and natural frequencies of hull structures appear usually between 0.5 Hz and 10 Hz. [4]

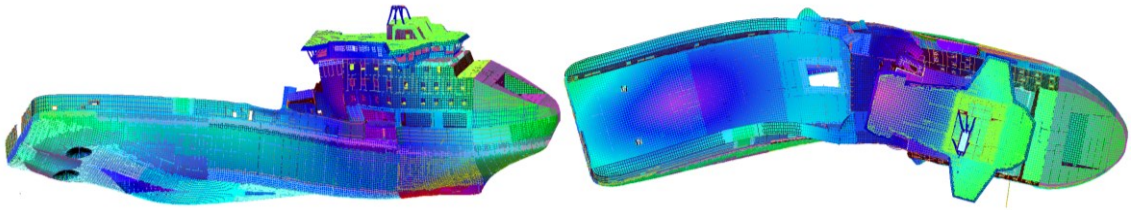

Figure 2. Coupled horizontal-torsional mode of a ship

3.2 Local Vibrations

While the natural frequencies of global modes typically occur below 10 Hz, the natural frequencies and modes of local structures can be found between 10 Hz and 50 Hz. The resonance of local structures can affect comfort of people on board especially in two ways, sensory vibrations of surrounding structures and structure-borne noise, which can be radiated from the structures at the hearing range of frequencies i.e. above 20 Hz. Also, local vibrations can also affect on the fatigue of the structures. [4]

For example, decks, bulkheads, platforms, handrails and foundations of equipment can be considered as local structures. Usually problematic vibrations arise at the local structures when strong inputs are received from the adjacent structure and these inputs are amplified by the resonance of the local structure. Also, vibrating equipment attached to local structures can act as input for exciting vibrating forces. [6]

Plate between stiffeners, stiffened plate bounded by solid supports or girder panels constrained by bulkheads can be considered as local structure panels that are fundamental local structural component in shipbuilding. In general, it is recommended that local structures should be designed the way that the natural frequencies of these structures are below 0.85 times the major exciting frequency or above 1.15 times the exciting frequency. [6]

In general, there are three different ways to design a structure what comes to the natural frequency, subcritical design where the natural frequency of the local structure is above the exciting frequency, supercritical design where natural frequencies of the local structure are below exciting frequency (Figure 3.) or by using frequency window method where natural frequencies of local structures are between excitation frequencies. Usually it is adequate to use subcritical design up to around 35 Hz i.e. where a resonant frequency of a local structure is above 35 Hz, and for higher frequencies use supercritical or frequency window method if needed. [4]

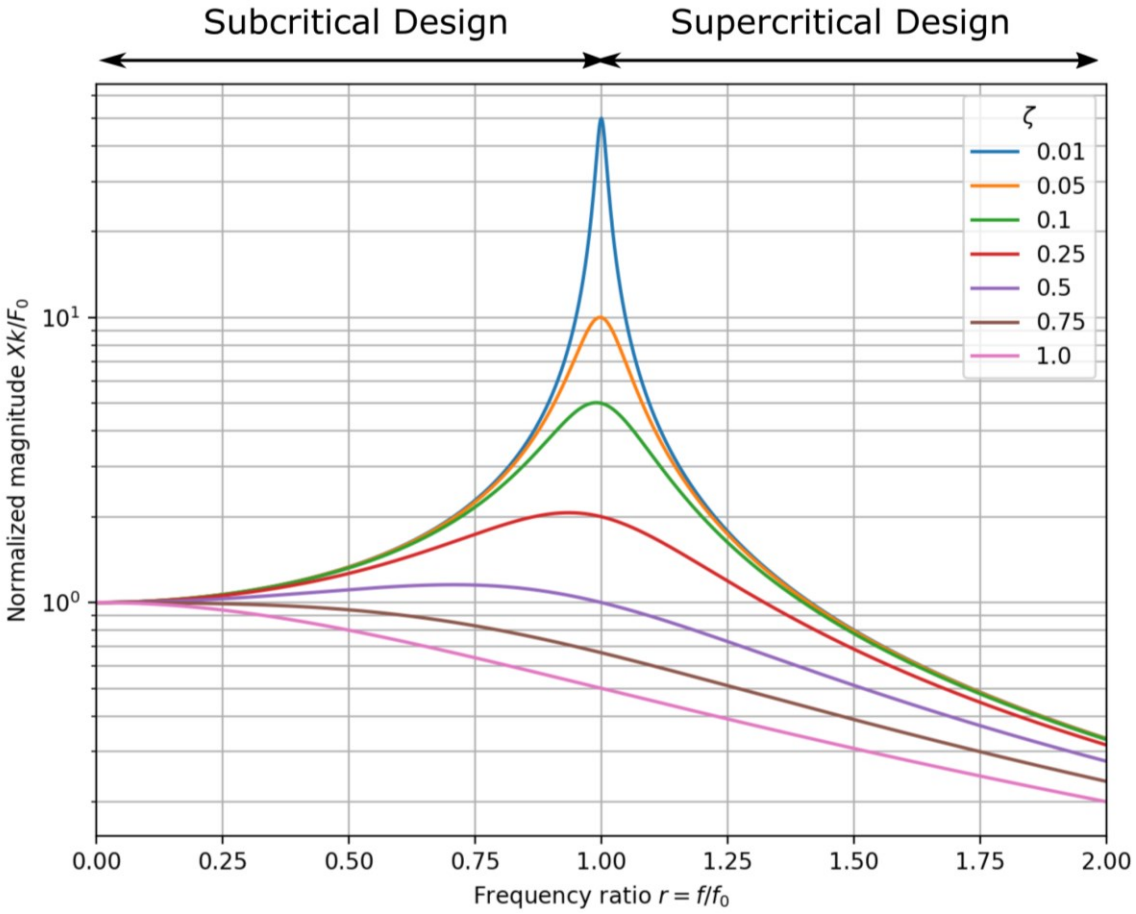

Figure 3. Subcritical and Supercritical design philosophies. Resonance occurs when frequency ratio r=1.

3.3 Vibration Sources

In this section, usual sources of vibration excitations are introduced. The most significant sources of vibrations in ships are low-speed diesel engines and the propeller excitation. Also, the seaway is a source of broadband excitations, however it usually excites primarily rigid body motions of ships. The exciting frequencies of the seaway are usually much smaller than the lowest natural frequencies of the ship hull, therefore it rarely excites the hull vibrations. [4]

3.3.1 Propeller Excitation

One type of propeller induced excitation is variating pressure on the ship hull and on the rudder due to the propeller blades displacement effect and cavitation of the propellers. Usually the cavitation effect is the dominant mechanism in generating vibration

excitation. The exciting frequency of the propeller is defined as blade frequency i.e. rotating frequency of the propeller times the number of blades. Vibration excitations also appear at the multiples of the blade frequency (higher harmonics) [4]. Fundamental excitation frequency and its harmonics can be described as:

$$f = k\frac{n\,z}{60}\ [Hz] \tag{1}$$

where, n is rotating frequency of propeller in rounds per minute, z is the number of blades, and k is a harmonic order i.e. 1, 2, 3,…,N.

The root cause in propeller induced vibration problems in general is the hull wake creating highly non-uniform flow field prior to propeller. Because of the complex nature of unsteady hydrodynamics of the non-uniform hull wake and the propeller operating in it, evaluating the excitation to ship structure is difficult [6]. Irregularities in fluid flow into the propeller i.e. level of non-uniformity in the hull wake, depends the form of the ship aft-body and positioning of the propeller. For example, in case of the typical full-form type tanker, the hull wake might be very non-uniform, with high velocity of the flow at the bottom and very low velocity at the top of the propeller. That creates conditions where considerable cavitation might occur at the top position of the blade. For the ships with the finer form, and for example ships with podded propulsion system, propellers are usually located in relatively uniform flow, leading to reasonable low dynamic forces. Two different components can be considered what comes to propeller excitation of the ship's hull, the non-cavitating component and the cavitating component. Ships with fixed pitch propeller, at the low speeds where negligible amount of cavitation occurs, the non-cavitating component will be dominant. This non-cavitating pressure excitation can be considered to have a sine wave form with the blade frequency. [7]

3.3.2 Engine Excitation

While engine manufacturers have done significant improvements in reducing vibration excitation of the engines during recent years, the excitations produced by the diesel engines are still another dominant source of ship vibration along with the propeller induced vibrations. Excitations generated by the diesel engines can be thought to have three force component and three moment components with the periodic nature. Usually forces acting along the longitudinal axis of the engines are considered to be zero and quite often also some other force and moment components are balanced to zero, but this varies between different engine designs and characteristics. Main sources of forces in reciprocating internal combustion engines are typically gas forces because of combustion process and inertia forces due to the accelerations of rotating and reciprocating engine components. External forces and moments acting on an engine are shown in Figure 4. [6]

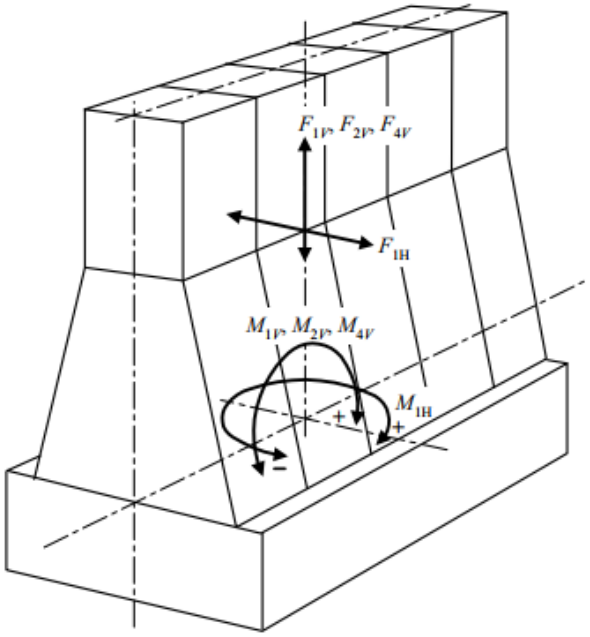

Figure 4. Forces and Moments acting on an engine foundation [6]

Similar to calculation of the excitation frequency of a propeller, the frequency of the excitation forces generated by a diesel engine can be calculated based on the running speed of the engine. In the case of two-stroke engines excitation frequencies appear at the rotational speed of the engine and its multiples. However, four-stroke engines also excite "half order" harmonics as well because in the four-stroke engines the running speed is twice the cycle speed [8]. The excitation frequencies can be described as:

$$f = k\frac{n}{60}\ [Hz] \tag{2}$$

where, n is running speed of the engine in revolutions per minute and k is a harmonic order i.e. $k = 1, 2, 3, \ldots, \mathrm{N}$ for two-stroke engines and $k = 0.5, 1, 1.5, 2, 2.5, 3 \ldots, \mathrm{N}$ for four-stroke engines.

Depending on the firing order and the number of cylinders, guide force couples might occur because of transverse reaction forces acting on crosshead guides, causing rocking moment and twisting moment of the engine body. The rocking is called H-couples, sometimes also called as H-mode or H-moment, and the twisting mode is called X-couples (or X-mode/moment) [6]. Illustration of the H- and X-mode are presented in Figure 5.

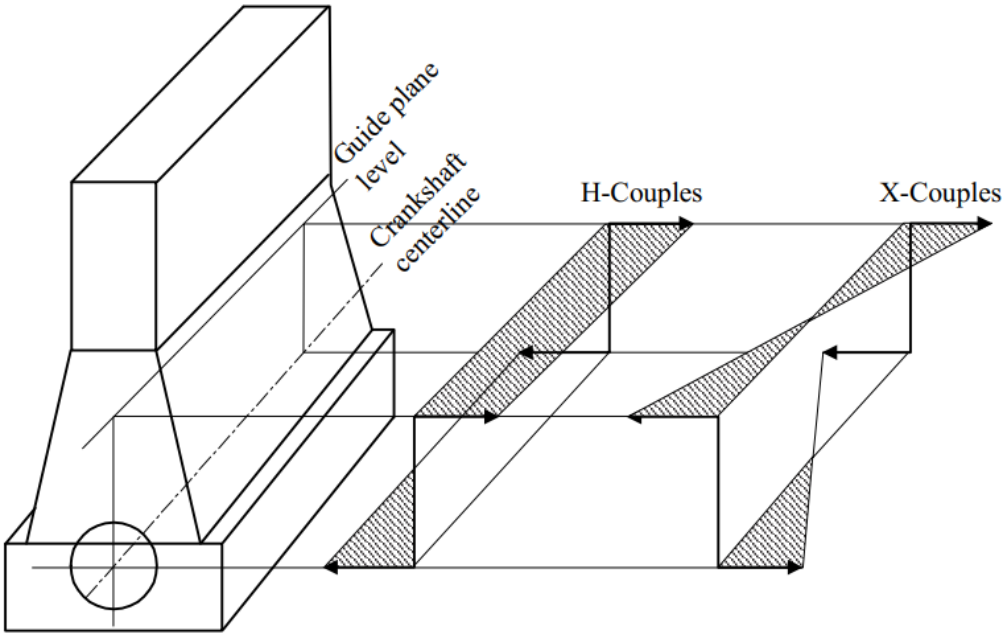

Figure 5. Guide force moments of an engine [6]

Different types of engines produce different type of excitations. Slow speed diesel engines that are often used in large cargo ships might have considerable imbalances at multiple frequencies and because of their large size and mass they are often fastened directly to surrounding structures causing the situation where vibratory excitations might be fully transmitted into the structures of the ship. Slow speed diesel engines usually operate roughly at the range of 70 to 130 RPM. These types of engines are usually connected directly to propeller shaft. Typically, the excitations of slow speed engines include both, horizontal and vertical first order moments, as well as vertical second order moments. Also, the rocking moment (H-couple) occurs at the engine firing frequency of the engine i.e. where the order number of exciting frequency equals with the number of cylinders. In addition to excitation mentioned above, also twisting moments around vertical axis (X-couple) occurs at multiple orders, however these modes do not affect externally to the surrounding structures and thus ship's hull due to their internal nature. [5]

Medium speed engines, which are used in ships presented in this thesis, from around 400 RPM up to 1200 RPM and high-speed engines above 1400 RPM are significantly lighter and smaller than slow speed engines and are normally mounted resiliently to the ship's structures. Compared to slow speed engines, the amount of external exciting forces generated by medium and high-speed engines, are considered to be really small and not to affect ship's global vibrations usually. [7]

3.3.3 Other Sources of Vibration

Even though the main sources of excitations are propulsion systems and main engines, also the seaway and fluid flow interaction with the hull can induce some amount of vibrations.

Usually exciting frequency of the seaway is way below lowest natural frequencies of the ship, therefore it mainly excites rigid body motions of the ship. Rigid body motions are illustrated in Figure 6.

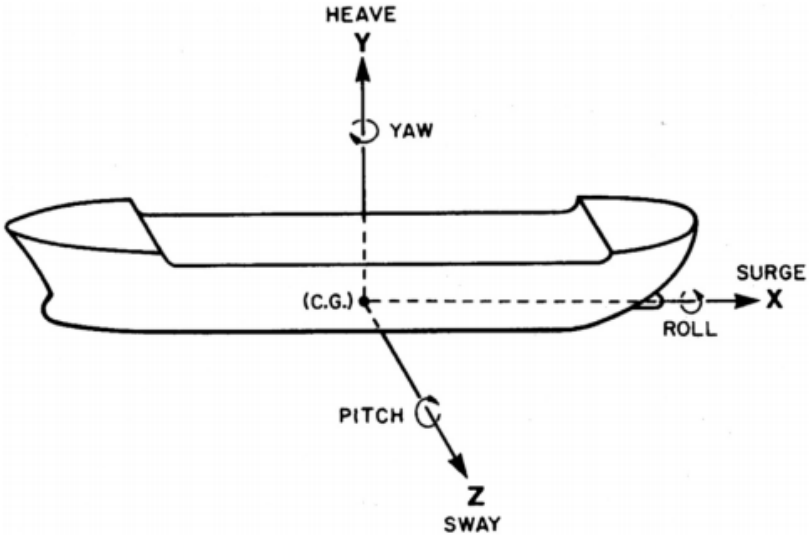

Figure 6. Rigid body motions of ships [9]

However, the seaway can excite vertical continuous vibrations of ship's hull, also called as springing, if the lowest natural frequency of the ship is less than 1 Hz, that is possible in case of very large ships. Also whipping, that is significant free vibrations of ship's hull, can occur due to the slamming of ship's hull. [4] Slamming happens when the fore of the ship hits the water. [9]

Also, the phenomena called vortex-induced vibrations might play a role in ship vibrations. Possible sources of vortex-induced vibration can be for instance A-brackets, fins and extended skegs. Typically, vibrations are generated due to the vortex shedding that happens when the fluid flow separates from the structure the way it creates pressure fluctuations on the hull of a ship making it vibrate. [4] [9]

4 Vibrations Analysis of Ships Using Finite Element Analysis

In this chapter the vibration analysis procedure of ship vibrations based on Finite Element Analysis is briefly looked into at the general level. The Finite Element Analysis methods presented in this chapter are based mainly on guidelines of different classification societies such as American Bureau of Shipping (ABS) [6], Lloyd's Register (LR) [7] and Germanischer Lloyd (GL) [10] that merged with the Norwegian classification society Det Norske Veritas (DNV) in 2013 forming a new DNV GL classification society.

The guidance notes on ship vibrations from American Bureau of Shipping provides an illustrative flowchart that shows main components of ship vibration analysis in one picture. The flowchart is presented in Figure 7.

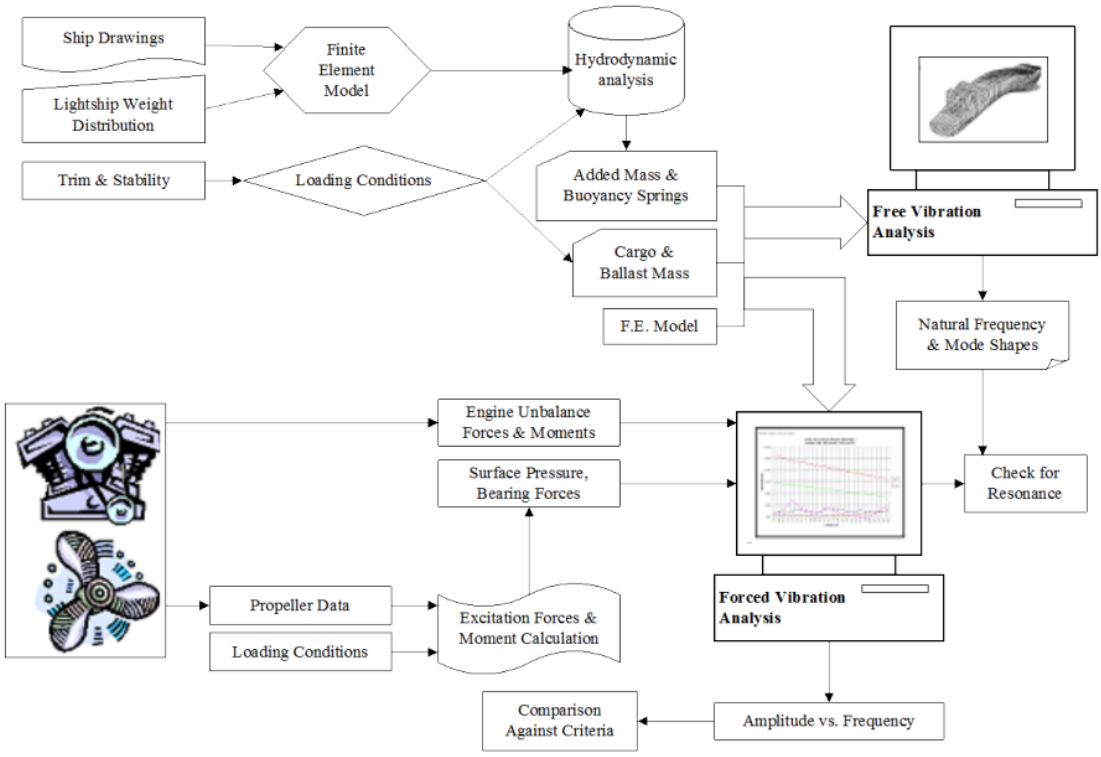

Figure 7. Flowchart of ship vibration analysis process [6]

A Finite Element Model is created from the scratch based on the drawings of the ship or alternatively it can be created from the 3D-model by using appropriate software if such model exists. The model will be complemented based on the known loading conditions and hydrodynamics. This includes for example surrounding water masses of the ship and masses from the cargo and ballast. At this point the model can be used for the natural frequency and eigenmode analysis. When more specific response analysis needs to be conducted, also quite detailed information about the excitations are required to conduct reasonable accurate forced vibration analysis. [6]

Even though classification societies do not really have mandatory rules about vibrations on ships, they do have optional class notations about habitability related vibration and noise standards. Also, for example International Standard Organisation (ISO) have

standards about mechanical vibrations on ships that provide some guidelines about acceptable vibration levels onboard as well as the standardized methods to measure these vibrations regarding to habitability on ships. [7]

4.1 Finite Element Model of a Ship

Different analysis types require different level of complexity of the model. If the analysis is carried out to find out only global modes and frequencies of the ship, quite coarse finite element mesh can be adequate to yield reasonable results if the idealization of the hull structure is done well. In a model like this, global mesh size can cover the length of three to four stiffener still produce reasonable results. However, some superstructures and some other details, like the stern of the ship might need finer mesh. [6]

For the analysis of local structural components and local structural panels, much finer mesh needs to be used compared to the analysis at the global level, that is up to six elements between stiffeners. Also, if only small section of the ship is modelled, some of the surrounding structures should be included into a model. [6]

In vibration analysis the mass of the ship and the distribution of the masses are really important issue. Heavy equipment should be modelled for example by using mass elements that are placed correctly. Center of the gravity of the FE-model should not differ more than 0.5 % of the total length of the ship from the designed value. In addition to masses from the general equipment, also other types of the masses should be modelled with the reasonable accuracy. These masses include for example outfitting, deck coverings, furniture and so on. [6] Two types of outfitting masses can be distinguished, masses with the distributed nature and masses which are concentrated. Distributed masses can be modelled for example by varying the material densities of the structural elements or by using non-structural mass properties. Even more detailed mass distribution can be used for example in the accommodation areas of passenger ships to produce more accurate results at these critical locations. The additional weight that comes from the outfitting masses can be quite significant, values between 50 to 100 kg/m^2 are fairly common. [7]

In addition to the sources of weight mentioned above, cargo, surrounding water masses and internal fluids such as fresh water, ballast and fuel, contributes vibrational behavior of the ship. Surrounding water masses creates an inertial effect on the dynamic behavior of the ship. Water masses can be added for example as mass elements on the ship's hull. This added mass from surrounding water can have the same order of the magnitude as the ship's mass and thus it plays a significant role in the vibrational behavior of the ship structures. [7]

4.2 Finite Element Analysis Types

Next, commonly used vibration analysis types based on Finite Element Analysis are introduced. Similar division is used as presented in the ship vibrations guidelines by American Bureau of Shipping [6], where analysis types are divided into free vibration analysis based on normal modes of the ship and forced response analysis of the ship.

4.2.1 Normal Modes Analysis

The normal modes analysis is used to find out the natural modes and frequencies of the ship structure. This is achieved by solving an eigenvalue problem where from the general

equation of motion (Equation 3) the eigenvalues, that is natural frequencies, and eigenvectors, that is mode shapes, are solved. [6]

$$M\ddot{\boldsymbol{x}} + C\dot{\boldsymbol{x}} + K\boldsymbol{x} = F \tag{3}$$

where M is a mass matrix, C is a damping matrix, K is a stiffness matrix, F is a force vector and $\boldsymbol{x}, \dot{\boldsymbol{x}}$ and $\ddot{\boldsymbol{x}}$ is displacement vector and its derivatives i.e. velocity and acceleration vectors.

For the free vibration problem, the damping and external forces are zero, thus the equation above reduces to the form:

$$M\ddot{\boldsymbol{x}} + K\boldsymbol{x} = 0 \tag{4}$$

and the solution to the eigenvalue problem will be:

$$(K - \omega^2 M)\,\boldsymbol{\phi} = 0 \tag{5}$$

where $\boldsymbol{\phi}$ is the mode shape vector and ω is the natural frequency. [6]

Normal mode analysis can be used to calculate the modes and natural frequencies of the ship, but it should be noted that it does not provide more detailed information about the response since the magnitudes of the eigenvectors are arbitrary. Calculated natural frequencies can be compared with known excitation frequencies to get some estimation of possible problematic behavior.

4.2.2 Forced Response Analysis

Forced response analysis is used to calculate the response of the ship's structure under the steady-state oscillating excitation. The harmonic loads representing excitations from engines and propulsion systems are applied into the finite element model. Basically, two different types of steady-state forced vibration analysis exists, a mode-based method and the direct method [6]. In the direct frequency response method, the coupled equations of motions are solved in terms of frequency of exciting force and in mode-based method mode shapes and natural frequencies of the structure are utilized in solution process. Utilizing mode shapes and natural frequencies calculated before forced response analysis could reduce the computational power needed to solve the problem. The following descriptions of analysis methods are based on the NX Nastran documentation. [11]

In Direct Frequency Response Analysis, the equation of motion of the system under harmonic excitation has the following form:

$$M\ddot{\boldsymbol{x}}(t) + C\dot{\boldsymbol{x}}(t) + K\boldsymbol{x}(t) = F(\omega)e^{i\omega t} \tag{6}$$

The harmonic motion is assumed to have the form:

$$\boldsymbol{x}(t) = \boldsymbol{u}(\omega)e^{i\omega t} \tag{7}$$

where $\boldsymbol{u}(\omega)$ is the complex displacement vector.

When $\boldsymbol{x}(t)$ and its derivatives $\dot{\boldsymbol{x}}(t)$ and $\ddot{\boldsymbol{x}}(t)$ are substituted into the Equation 6 and divided by $e^{i\omega t}$, the equation of motion simplifies to:

$$[-\omega^2 M + i\omega C + K]\boldsymbol{u}(\omega) = F(\omega) \quad (8)$$

From the Equation 8, the frequency response can be calculated by solving the equation for $\boldsymbol{u}(\omega)$ with known excitation force $F(\omega)$. [11]

In Modal Frequency Response analysis, the mode shapes are used to uncouple the equations of motion. Utilizing calculated modes can reduce the computational cost of the analysis, especially if mode shapes are already solved in normal mode analysis prior to forced response analysis. The modal frequency response analysis uses same form of equations of motion (Equation 6) and same assumed harmonic solution for displacement (7) as direct frequency response analysis. By ignoring the damping term and introducing response transform from physical $\boldsymbol{u}(\omega)$ to modal coordinates $\xi(\omega)$:

$$\boldsymbol{x}(t) = \boldsymbol{\phi}\, \xi(\omega) e^{i\omega t} \quad (9)$$

the Equation 6 gets the following form:

$$-\omega^2 M\, \boldsymbol{\phi}\, \xi(\omega) + K\, \boldsymbol{\phi}\, \xi(\omega) = F(\omega) \quad (10)$$

At the current form the equations of system of Equations 10 are coupled. Pre-multiplication by the transpose of $\boldsymbol{\phi}$ produces the uncoupled form of the equation system:

$$-\omega^2 \boldsymbol{\phi}^T M\, \boldsymbol{\phi}\, \xi(\omega) + \boldsymbol{\phi}^T K\, \boldsymbol{\phi}\, \xi(\omega) = \boldsymbol{\phi}^T F(\omega) \quad (11)$$

where $\boldsymbol{\phi}^T M\, \boldsymbol{\phi}$ is a modal mass matrix, $\boldsymbol{\phi}^T K\, \boldsymbol{\phi}$ is a modal stiffness matrix and $\boldsymbol{\phi}^T F$ is a modal force vector.

Equation 11 can be presented in the single degree of freedom form as in:

$$-\omega^2\, m_i\, \xi_i(\omega) + k_i\, \xi_i(\omega) = f_i(\omega) \quad (12)$$

where m_i, k_i and f_i are the modal mass, stiffness and force of the i^{th} mode, respectively. The modal responses $\xi_i(\omega)$ can be translated to the physical responses by using Equation 9.

5 Soundproofing Floor Structures

In the shipbuilding applications, soundproofing floor structures like floating floors are used to reduce noise and vibration levels especially in the ship cabins at the critical locations, for example above engine rooms and other areas with high intensity noise and vibration sources [12]. To obtain the most optimal noise reduction properties, the floating floor structure is usually complemented with visco-elastic resilient layers and additional steel plates to create so called combined floor structure [13].

In general, noise and vibration reducing floor structures can be divided in three categories, floating floors, visco-elastic floors and combined floating and visco-elastic floors. Combined floor structures are typically used in marine applications, when floating floors are more common in civil engineering applications where sound insulation is especially needed. Even though these three categories exist, quite often the term floating floor is used when referred any of these floor structures.

Next, couple concepts that are used to describe the performance of soundproofing floor structures are introduced. These are the sound reduction index R, the transmission loss TL_v and the insertion loss IL_v. [14]

- Sound reduction index R describes the level of airborne sound insulation
- Transmission loss TL_v describes the velocity difference between deck plating and floor plating in sound proofing floor structures.
- Transmission loss TL describes the difference in sound pressure levels between the source and the receiving room.
- Insertion loss IL_v describes the velocity difference of the floor with and without the soundproofing floor structure, in other words, how much the sound proofing floor structure improves the level of vibrations compared to the bare deck situation.

The concepts above are used to describe the performance of different floor structures in forthcoming chapters.

5.1 Floating Floors

In general, a floating floor consists of a base floor, an elastic interlayer and a floor on the top of the elastic interlayer. The operating principle of floating floors is based on the isolation of the floor from the surrounding structures. In naval applications this is often carried out by using a slab of mineral wool between the deck plating and the actual floor plate with flooring. Using a floating floor can improve significantly impact noise isolation and reduce airborne sound transmission through structures. [15]

Noise reduction properties of floating floor structures appear at the frequencies above the natural frequency of the floating floor structure. Typically, noise reduction gets better when the frequency of noise gets higher. An example of sound reduction properties of a floating floor construction (Figure 8) is presented in Figure 9.

The floating floor construction in Figure 8, contains 6 mm thick steel deck plating, 50 mm thick layer of SeaRox SL 436 mineral wool with the density of 140 kg/m^3 and two layers of steel plates glued together on the top of the mineral wool layer. The measured sound reduction index of the floating floor structure is presented in Figure 9.

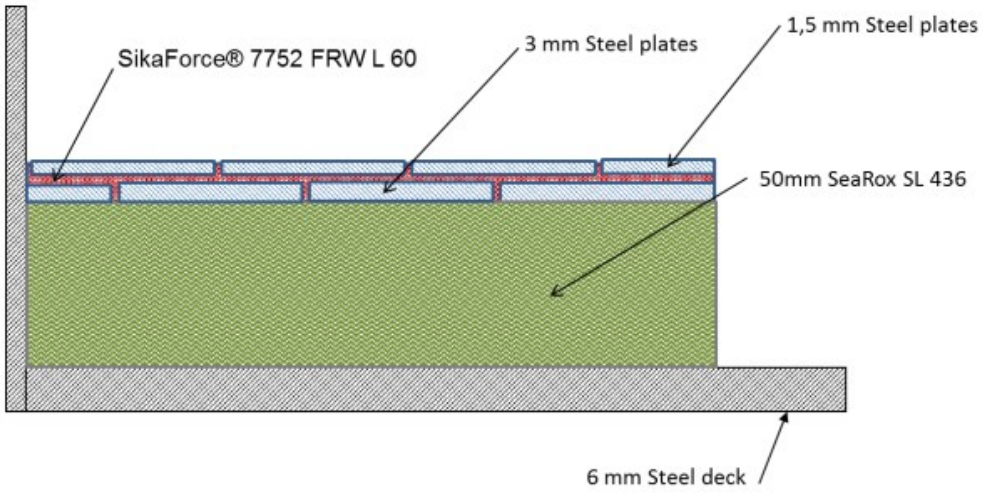

Figure 8. Sikafloor Marine FLF Type 8.2 construction. [14]

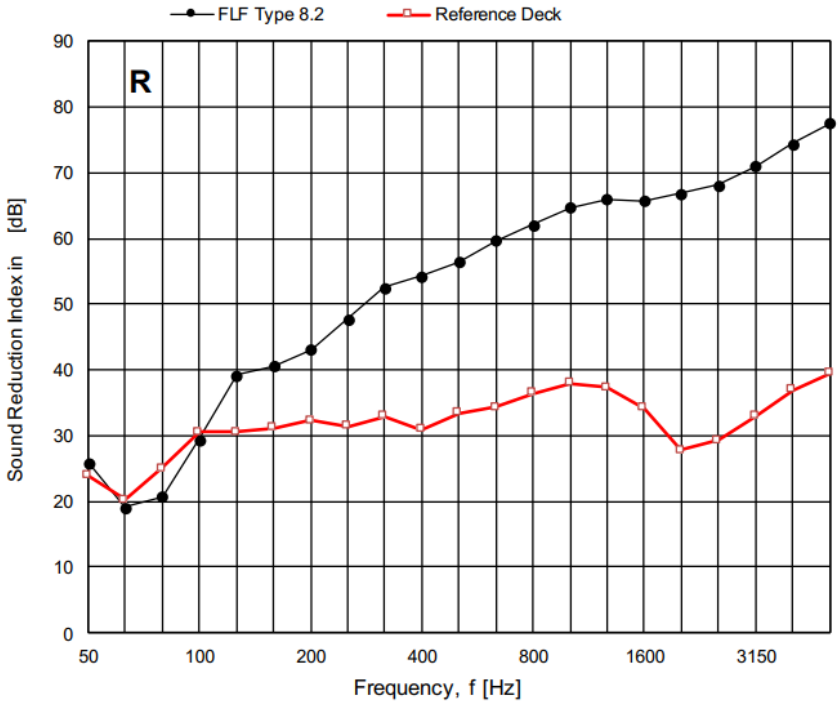

Frequency f [Hz]	R 1/3-octave [dB]
50	25.9
63	19.0
80	20.8
100	29.4
125	39.2
160	40.5
200	43.2
250	47.8
315	52.5
400	54.3
500	56.4
630	59.7
800	62.0
1000	64.7
1250	65.9
1600	65.8
2000	66.8
2500	68.2
3150	71.0
4000	74.4
5000	77.6

Figure 9. Measured sound reduction index of the FLF Type 8.2 compared to bare deck composition [14]

In Figure 10, the measured insertion loss of the example floating floor is presented. It shows how much the vibration velocity of the floor is reduced by using the floating floor compared to the bare deck condition.

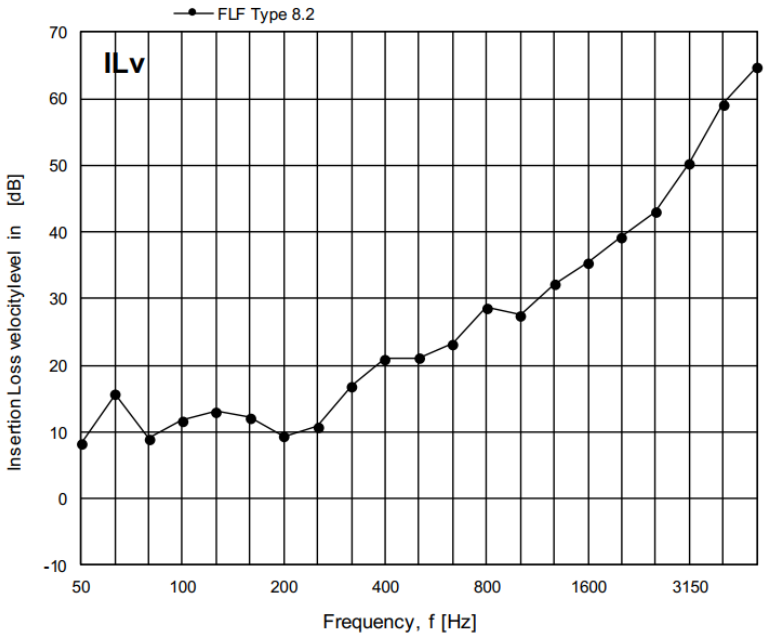

Frequency f [Hz]	ILv 1/3-octave [dB]
50	8.1
63	15.7
80	8.9
100	11.7
125	13.1
160	12.2
200	9.4
250	10.8
315	16.9
400	21.0
500	21.1
630	23.2
800	28.7
1000	27.6
1250	32.2
1600	35.4
2000	39.2
2500	43.0
3150	50.4
4000	59.1
5000	64.8

Figure 10. Measured Insertion Loss IL_v of the FLF Type 8.2 floating floor [14]

Finally, the transmission loss TL_v (velocity) of the FLF Type 8.2 floating floor structure is shown in Figure 11 and the transmission loss TL (sound pressure) is shown in Figure 12.

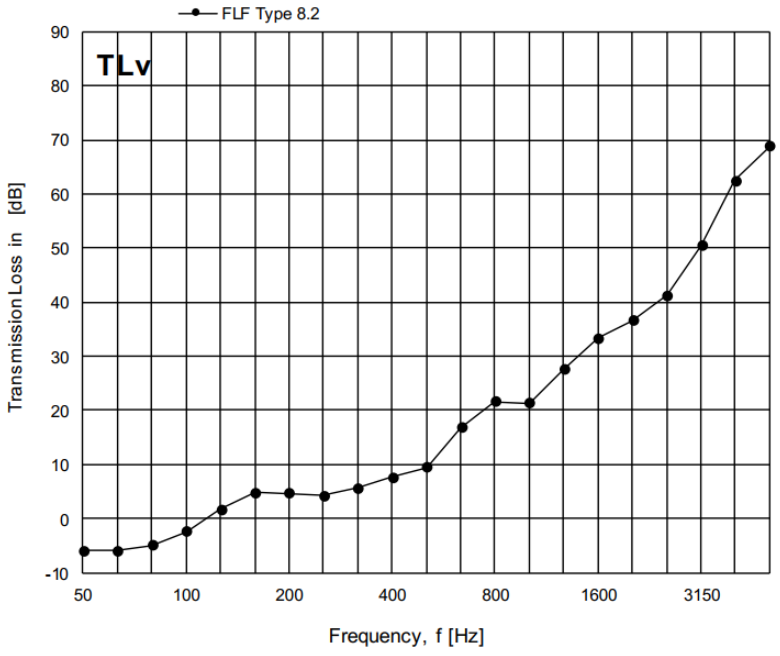

Frequency f [Hz]	TLv 1/3-octave [dB]
50	-5.9
63	-5.9
80	-5.0
100	-2.4
125	1.6
160	4.7
200	4.7
250	4.2
315	5.6
400	7.6
500	9.5
630	16.9
800	21.7
1000	21.3
1250	27.6
1600	33.4
2000	36.7
2500	41.2
3150	50.5
4000	62.5
5000	68.8

Figure 11. Measured Transmission Loss TL_v of the FLF Type 8.2 floating floor [14]

In Figure 11, quite typical behavior of floating floor can be seen, where the floating floor might actually increase the vibration levels at the lower frequencies.

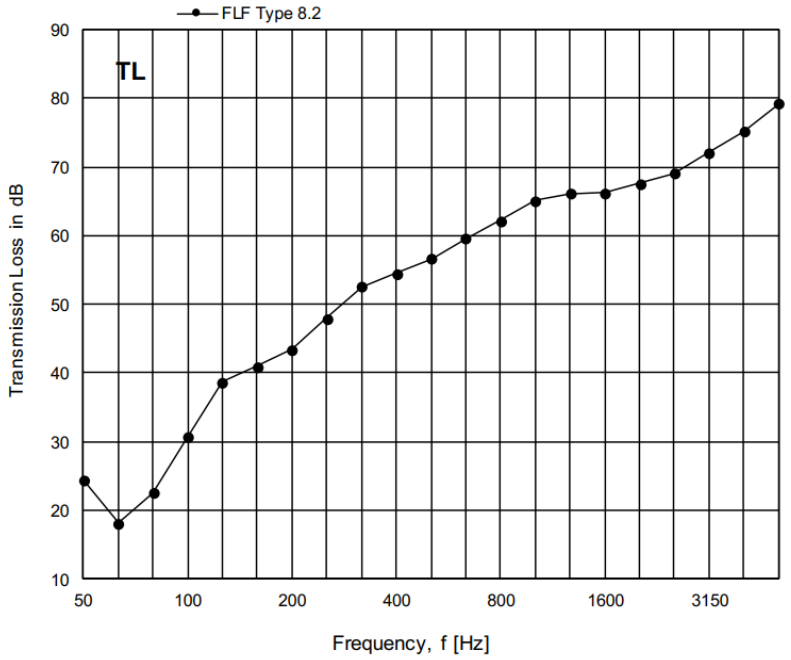

Frequency f [Hz]	TL 1/3-octave [dB]
50	24.4
63	18.2
80	22.6
100	30.8
125	38.7
160	40.9
200	43.5
250	48.0
315	52.6
400	54.5
500	56.7
630	59.6
800	62.3
1000	65.1
1250	66.2
1600	66.3
2000	67.6
2500	69.1
3150	72.1
4000	75.2
5000	79.3

Figure 12. Measured Transmission Loss TL of the FLF Type 8.2 floating floor [14]

5.2 Visco-Elastic Floors

Another type of a soundproofing floor structure is a visco-elastic floor. While floating floors can be considered to attain their soundproofing properties due to the isolation from surrounding structures, the operation of visco-elastic floors is based on the damping of vibrations. Vibrations induces shearing between visco-elastic layer and constraining layer that converts the kinetic energy of vibrations into heat [13]. Unlike floating floor structures, visco-elastic floors provide noise reduction properties also at the lower frequencies. [16]

Next, soundproofing and vibration reduction properties of an example visco-elastic floor structure are presented in the same manner as in the chapter about floating floors. The example floor is Sikafloor Marine Visco EM 5 constrained damped construction (Figure 13). Above the 6 mm steel deck there is the 2 mm layer of VEM X visco-elastic vibration damping mortar. The damping layer is constrained by using 3 mm steel plates on the top of it. [17]

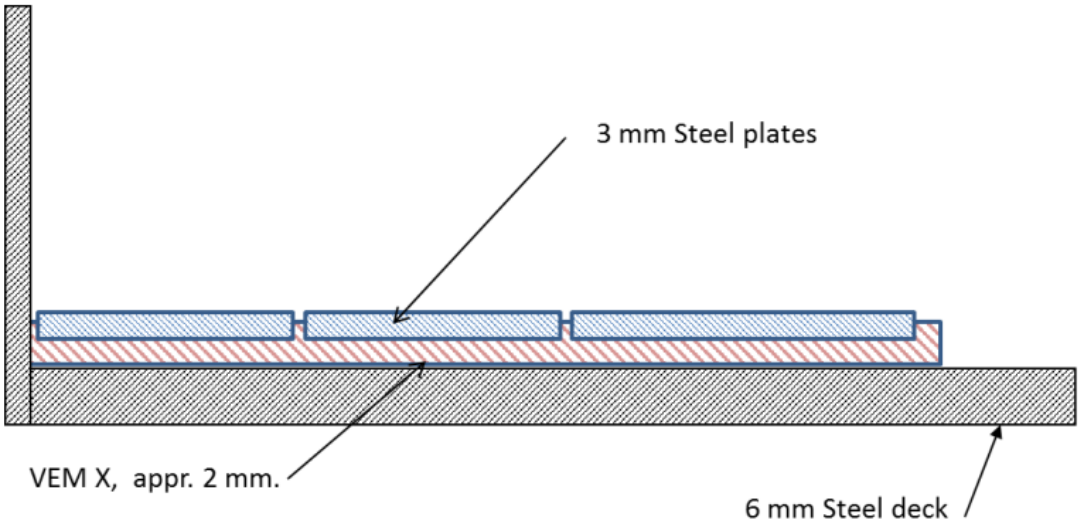

Figure 13. Sikafloor Marine Visco EM 5 construction

The measured sound reduction index of the visco-elastic floor structure is presented in Figure 14. From Figure 14 it can be seen, how visco-elastic construction reduces sound level also at the lower frequencies unlike floating floors. However, the amount of sound reduction does not increase much as in the floating floor construction as the frequency gets higher.

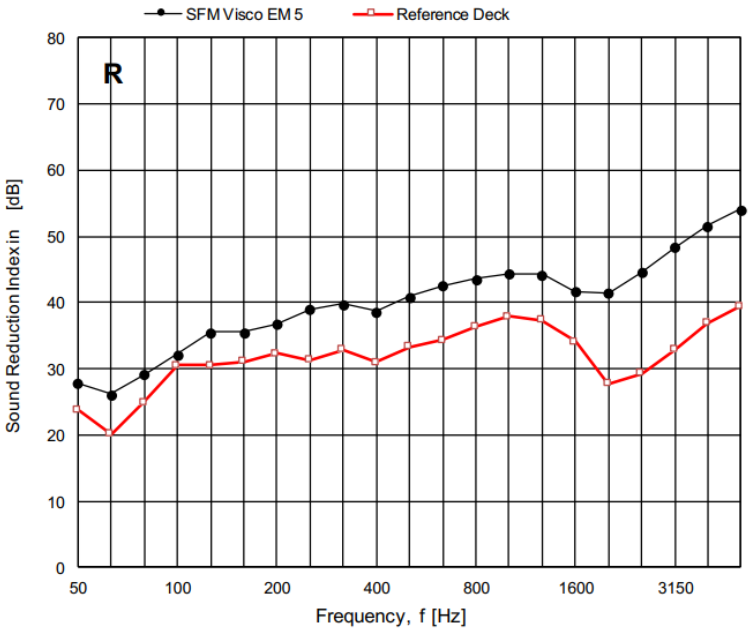

Frequency f [Hz]	R 1/3-octave [dB]
50	27.9
63	26.2
80	29.2
100	32.3
125	35.5
160	35.6
200	36.8
250	39.0
315	39.8
400	38.6
500	40.9
630	42.6
800	43.6
1000	44.4
1250	44.3
1600	41.7
2000	41.5
2500	44.7
3150	48.4
4000	51.7
5000	54.1

Figure 14. Measured sound reduction index of the Sikafloor Marine Visco EM 5 floor compared to bare deck composition [17]

In Figure 15, the measured insertion loss of the example visco-elastic floor is presented. It shows how much the vibration velocity of the floor is reduced by using the visco-elastic construction compared to the bare deck condition. It shows that the visco-elastic floor provides approximately constant damping through the frequency range.

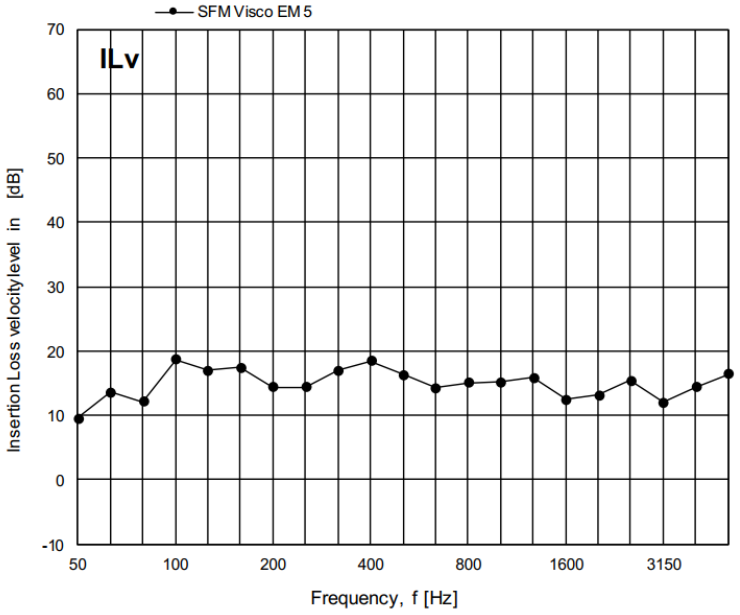

Frequency f [Hz]	ILv 1/3-octave [dB]
50	9.5
63	13.6
80	12.1
100	18.6
125	17.0
160	17.5
200	14.3
250	14.4
315	17.0
400	18.4
500	16.3
630	14.2
800	15.1
1000	15.2
1250	15.8
1600	12.5
2000	13.1
2500	15.4
3150	12.0
4000	14.4
5000	16.4

Figure 15. Measured Insertion Loss IL_v of the Sikafloor Marine Visco EM 5 floor construction [17]

The transmission loss TL of the Sikafloor Marine Visco EM 5 constrained damped construction is shown in Figure 16.

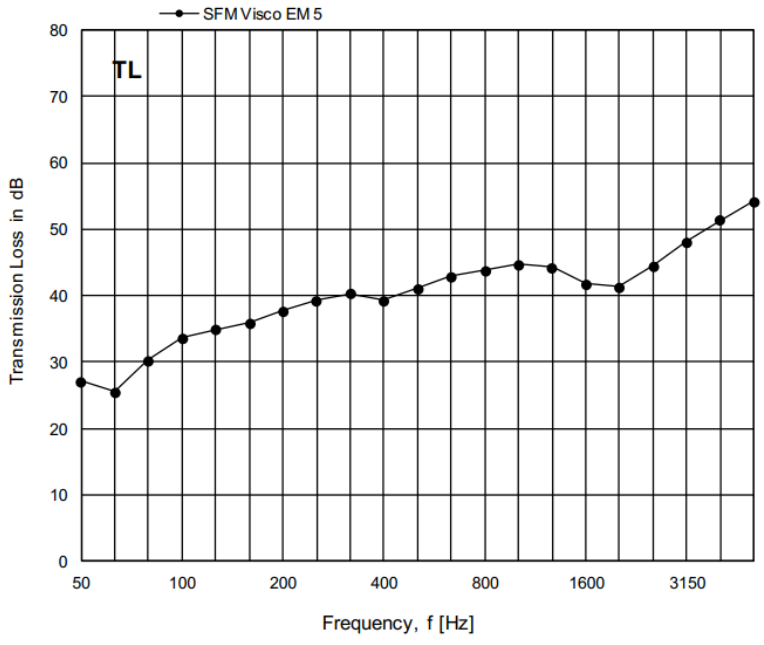

Frequency f [Hz]	TL 1/3-octave [dB]
50	27.1
63	25.6
80	30.3
100	33.6
125	34.9
160	35.9
200	37.7
250	39.4
315	40.3
400	39.2
500	41.2
630	42.8
800	43.9
1000	44.7
1250	44.3
1600	41.8
2000	41.3
2500	44.5
3150	48.1
4000	51.4
5000	54.2

Figure 16. Measured Transmission Loss TL of the Sikafloor Marine Visco EM 5 floor construction [17]

When transmission losses in sound pressure levels are compared between the floating floor structure (Figure 12) and the vísco-elastic floor (Figure 16), it can be seen that at the lower frequencies, below 100 Hz, the visco-elastic floor provides better sound

reduction, but after some point around 100-125 Hz, the floating floor gives the better level of soundproofing.

5.3 Combination Floors

Combination floors are used to obtain best parts from both, floating floors and visco-elastic floors. There are dozens of different compositions available at the markets from different manufacturers. In general, a combination floor consists one floating floor and one or two visco-elastic floors. Quite usual composition has a visco-elastic floor on the top of deck plating, and on the top of that there is a floating floor and another visco-elastic floor. [16]

The combination floor that is used as an example is the Sikafloor Marine Visco-FLF Type 26. The composition can be seen in Figure 17.

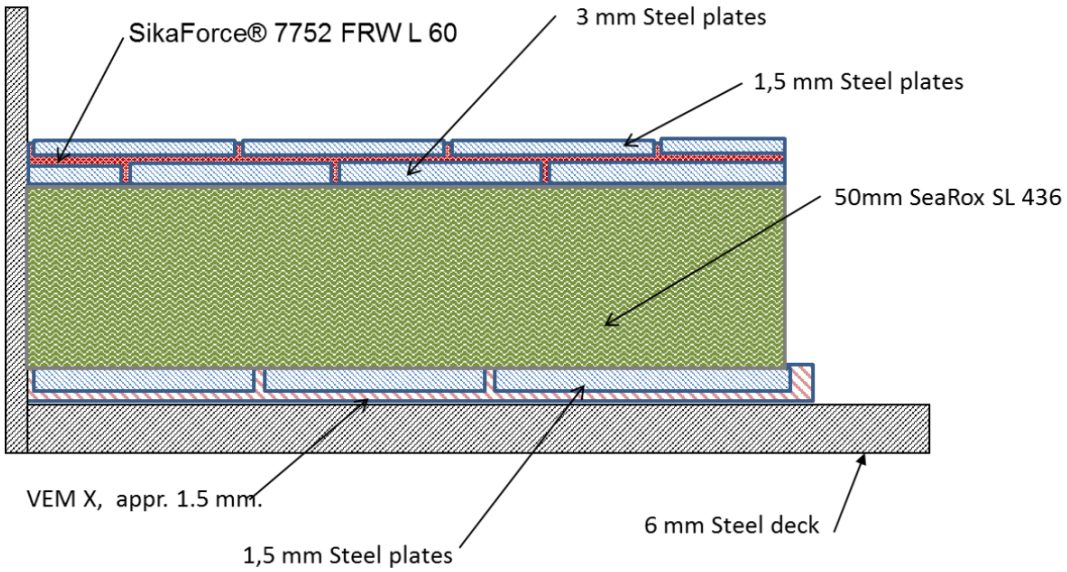

Figure 17. Sikafloor Marine Visco-FLF Type 26 construction [18]

The measured sound reduction index of the combination floor structure is presented in Figure 18.

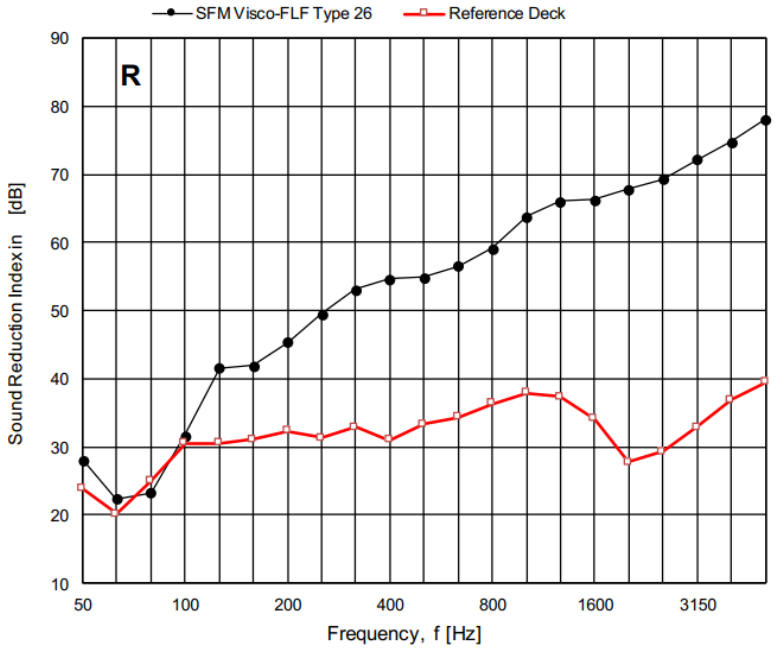

Frequency f [Hz]	R 1/3-octave [dB]
50	28.0
63	22.4
80	23.3
100	31.6
125	41.6
160	41.9
200	45.4
250	49.5
315	53.1
400	54.7
500	54.9
630	56.6
800	59.1
1000	63.8
1250	66.1
1600	66.3
2000	67.9
2500	69.4
3150	72.2
4000	74.8
5000	78.1

Figure 18. Measured sound reduction index of the Sikafloor Marine Visco-FLF Type 26 compared to bare deck composition [18]

In Figure 19, the measured insertion loss of the example combination floor is presented.

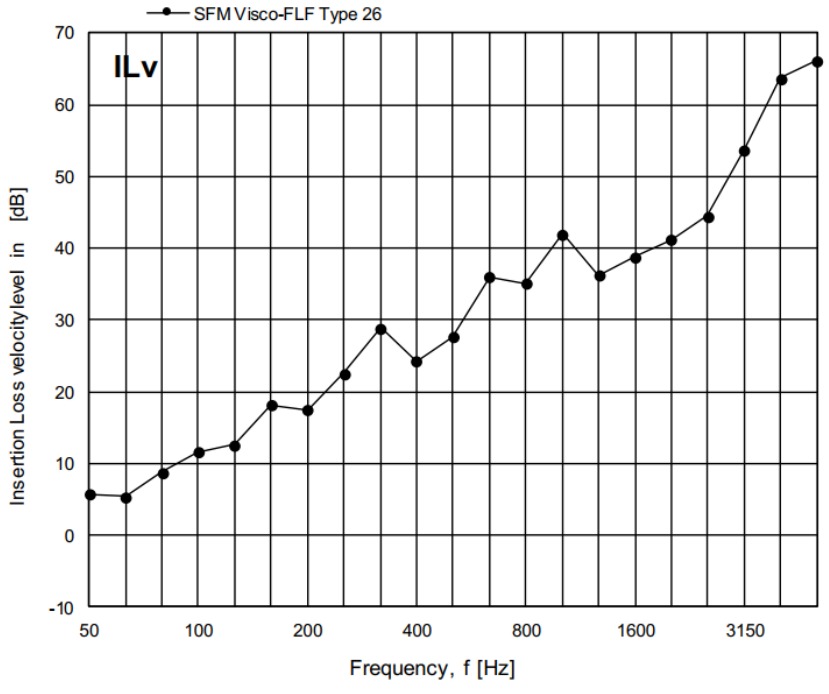

Frequency f [Hz]	ILv 1/3-octave [dB]
50	5.7
63	5.3
80	8.8
100	11.5
125	12.6
160	18.1
200	17.5
250	22.5
315	28.8
400	24.3
500	27.6
630	36.0
800	35.1
1000	41.9
1250	36.2
1600	38.8
2000	41.2
2500	44.4
3150	53.8
4000	63.7
5000	66.1

Figure 19. Measured Insertion Loss ILv of the Sikafloor Marine Visco-FLF Type 26 construction [18]

In Figure 20 and Figure 21, the transmission losses TLv and TL are shown, respectively.

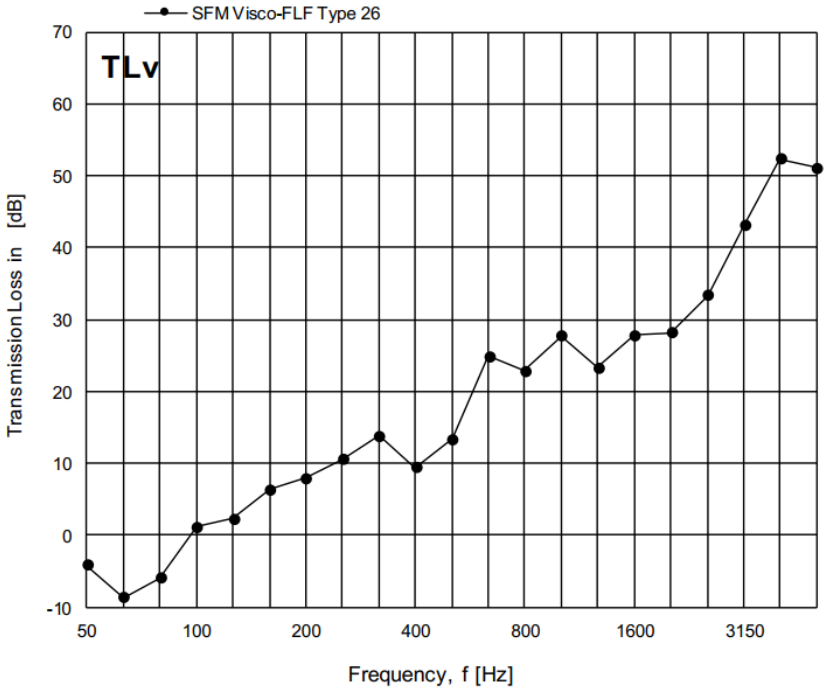

Frequency f [Hz]	TLv 1/3-octave [dB]
50	-4.1
63	-8.7
80	-5.9
100	1.1
125	2.3
160	6.4
200	7.9
250	10.6
315	13.9
400	9.4
500	13.4
630	24.9
800	22.8
1000	27.7
1250	23.3
1600	27.9
2000	28.2
2500	33.4
3150	43.1
4000	52.3
5000	51.1

Figure 20. Measured Transmission Loss TL_v of the Sikafloor Marine Visco-FLF Type 26 construction [18]

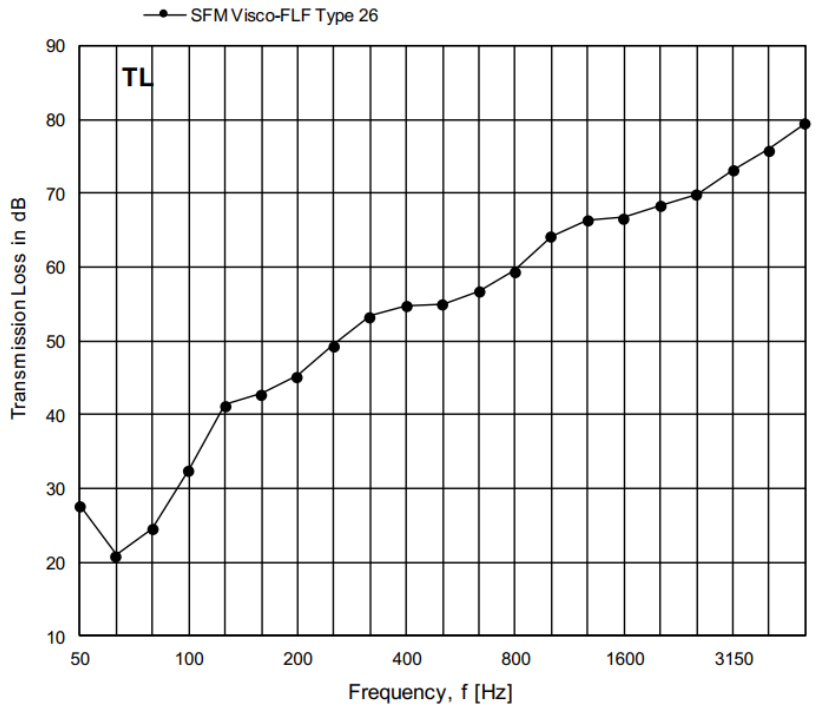

Frequency f [Hz]	TL 1/3-octave [dB]
50	27.8
63	20.9
80	24.5
100	32.6
125	41.3
160	42.9
200	45.3
250	49.4
315	53.4
400	54.8
500	55.0
630	56.8
800	59.5
1000	64.2
1250	66.5
1600	66.8
2000	68.4
2500	69.9
3150	73.2
4000	76.0
5000	0.0

Figure 21. Measured Transmission Loss TL of the Sikafloor Marine Visco-FLF Type 26 construction [18]

From the soundproofing point of view, the combination floor provides good reduction in noise levels at the whole frequency range, from low frequencies to higher frequencies. However, as the comparison between Figure 20 and Figure 21 shows, similarly to floating

floor only constructions, the vibration levels might increase through the floor structure even though the amount of noise is reduced. This might be rising some comfort issues especially if the accommodation areas are considered.

5.4 Dynamic Stiffness of Resilient Material in Floating Floors

The dynamic stiffness of resilient material, like mineral wool in floating floors, is one of the parameters that is used to estimate sound insulation and dynamic properties of soundproofing floor structures. In general, it is given by a manufacturer in the datasheet of the material and can be used to estimate the natural frequency of the floating floor construction.

The testing procedure to determining the dynamic stiffness is specified by the the European Standard EN 29052-1:1992 [19]. The dynamic stiffness s' describes the ratio between the dynamic response (displacement) and the applied dynamic force:

$$s' = \frac{F/S}{\Delta d}[N/m^3] \tag{13}$$

where F is the dynamic force acting on the test specimen, S is the area of the test specimen and Δd is the dynamic change in thickness of the resilient material due to the applied dynamic force.

Dynamic stiffness is used to calculate the natural frequency of a floating floor structure as described in:

$$f_0 = \frac{1}{2\pi}\sqrt{\frac{s'}{m'}} \tag{14}$$

where $s'$is the dynamic stiffness per unit area and m' is the total mass per unit area on the top of a resilient material. [19]

The dynamic stiffness of a test piece s'_t is determined by exciting the sample-load plate system as seen in Figure 22 by using a sinusoidal, a white noise or a pulse signal. When the resonant frequency of a system is found, the dynamic stiffness can be calculated from the Equation 15 when the total mass of a load plate is known. [19]

$$s'_t = 4\,\pi^2\,m'_t\,f_r^2 \tag{15}$$

where m'_t is the total mass per area on the test piece and f_r is the extrapolated resonant frequency.

The extrapolated resonant frequency f_r is used if the measured resonant frequency depends on the amplitude of the exciting force. For instance, for the materials with the estimated dynamic stiffness below $50\ MN/m^3$, excitation forces between 0.1 N and 0.4 N should be used and at least three different measurements with different applied forces

are needed. Based on these measurements the resonant frequency f_r is extrapolated at the zero force amplitude.

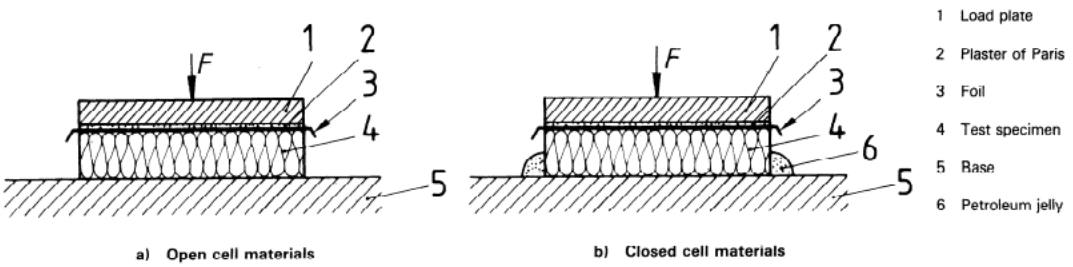

Figure 22. One example of a measurement setup defined in ISO 9052-1:1989 [19]

Even though the resonant frequency of a floating floor structure can be estimated by using the dynamic stiffness value given by the manufacturer of a resilient material, it does not provide any practical means to evaluate the response (displacement, acceleration etc.) of a floating floor system.

5.5 Floor Structure Under Investigation

In both cases where excessive vibrations were detected, the combined floor structures are similar with each other and the basic structure is shown in Figure 23. On the top of a 6 mm thick steel deck there is a 1 mm visco-elastic layer and 1.5 mm thick steel plate. On the top of that is the floating floor structure that consists 50 mm thick slab of mineral wool with the density of 140 kgm^{-3} and a 5 mm thick steel plate on the top of wool layer. Usually some kind of flooring is applied on the surface of floating floor, for example inside the cabins of NB 511 there are a smoothing layer and vinyl flooring.

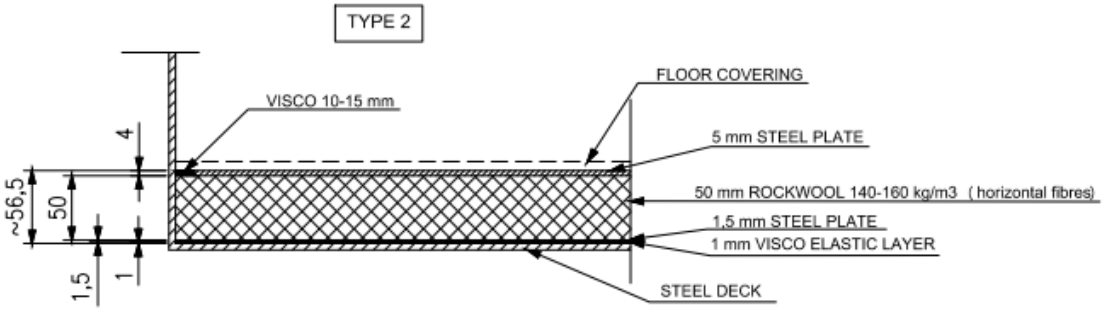

Figure 23. The structure of the combination floor used in the areas where vibration problems occurred in ships NB 506 and NB 511

In the aft wheelhouse area of the NB506, on the top of the quite similar combined floor structure as shown in Figure 23 there is raised floor structure as can be seen in the Figure 24. The wheelhouse flooring is raised from the floating floor by using 10 mm thick steel slab with the diameter of 100 mm and 50 mm x 50 mm x 5 mm L-profile.

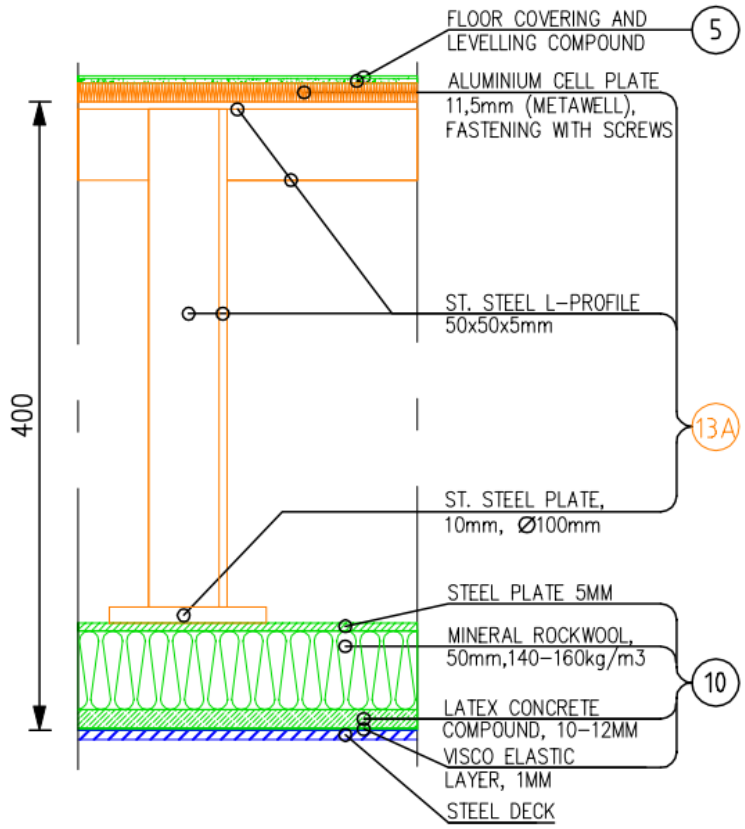

Figure 24. Floor structure at the wheelhouse of NB 506.

Even though this specific combination floor structure is present in both studied cases, it should be noted that in most cases the floor structure functions as intended, and vibration problems does not occur. Thus, it cannot be said that the floor structure itself is problematic, more like the problematic behavior arises due to the complex dynamic behavior of composition of different structures and the excitations acting on the system.

6 Preliminary Study of Modelling Methods

In this chapter different possible modelling methods that were considered during the project are investigated briefly. Three different modelling approaches are looked into in this preliminary study phase, a simple mathematical model of a floating floor structure, modelling methods based on the Finite Element Analysis and finally modelling based on modal analysis of a floating floor structure.

6.1 Simple Mathematical Model

There are some papers where floating floor structures are modelled using fairly simple mathematical models. These models are used for example to predict the insertion loss of floating floor structures in ships [12], to evaluate impact sound insulation in dwellings [20] and to analyze structure-borne noise in ship cabins with combined floating and viscoelastic floors [21].

Also, the mineral wool manufacturers use often the concept of dynamic stiffness to estimate the natural frequencies of floating floor structures. The dynamic stiffness of the mineral wool is based on the measurements and can be used to evaluate the natural frequency of a floating floor when the dynamic stiffness of the wool and mass per area on the top of the mineral wool slab are known. Even though this method provides quite straightforward method to approximate the natural frequency of the floating floor structure, it does not provide any practical means to evaluate the response of the structure i.e. displacements, accelerations or velocities at the top of floating floor. [19]

Even though it would be possible to model a floating floor structure by using the basic concepts of vibration dynamics that replicates behavior of a real structure reasonable accurately, at least if the degrees of freedom are limited enough, a downside would be that the model cannot be used easily in the global analysis. The model would represent only a small part of the whole ship and excitations must be defined at the local level.

6.2 Finite Element Modelling Approaches

Finite element- models are already used to evaluate the behavior of the ship at the global level, thus using the same models with appropriate modifications would be a tempting approach. Two different main approaches can be considered what comes to FE-analysis, implementing the floating floor structure into the global model or using a submodel of the area of interest. Including the floating floor structure into the global model could increase the size of the model too much, hence a submodel of the problematic area could be a better option, even though it requires additional modelling. Using a submodel creates an additional problem what comes to the excitation of the model. It is quite straightforward to apply excitations to the global model, however, if a submodel is used excitations have to be defined at the local level with reasonable accuracy.

Idealization of the structures is something that is widely used to simplify complex ship structures to achieve lower computational costs of the FE-analysis. One way to reduce the size of the FE-model by idealization is to include secondary stiffeners into the plate or shell element formulation to achieve behavior of the original structure accurately enough. Another similar method is called lumping of the stiffeners, where secondary stiffeners are incorporated into the beam elements at the edges of the plate elements. [22] At first, idealization of the floating floor structures by using shell elements with modified

properties to achieve desired behavior could sound like a promising approach to study. However, floating floors have significant out of plane behavior i.e. different response at the bottom and at the top of the structure, that cannot be captured easily by using only plate elements. For this same reason, also plate elements with composite material properties can be excluded from the list of appropriate modelling methods of floating floor structures. Another issue with composite plate elements could be the sandwich structure-behavior of these elements, where different layers are constrained with each other at their contact interface as well as at the outer boundaries of the plate.

Due to the significant out of plane behavior mentioned above, modelling the floating floor structures only by plate elements might not produce results reasonable enough. If submodeling method is used, the layer of mineral wool could be modeled as solid elements or even by using spring-dashpot elements that are widely available in commercial finite element software, without increasing the size of the model too much.

Another quite significant problem in the finite element modelling approach is the material model of the mineral wool. There is surprisingly little information about the mechanical behavior of mineral wool slabs available in general. This is understandable since usually for example thermal and sound insulation properties are more important when considered the use of mineral wool materials.

6.3 Modal Analysis

The third option was to study the dynamic behavior of floating floor structures and mineral wool slabs by using actual measurements and the means of experimental modal analysis. The modal analysis is a way to determine dynamic characteristics of the system, such as mode shapes, natural frequencies and damping factors, and utilize these features to the derivation of a mathematical model of the dynamic system. [23]

The modal analysis process of this approach could be based on the concept of dynamic stiffness of resilient materials used in floating floor structures that was introduced in Chapter 5.4. A method to measure and define an ‘improved dynamic stiffness’ of a resilient material could be developed. It could be something very similar to measurements of dynamic stiffness but using wider range of loading conditions and frequency range. The outcome of the measurements and modal analysis could be a transfer function or set of transfer functions that could be used to evaluate the response of the floating floor system in frequency domain when the loading function is known. A representation of a simple version this kind of system is shown in Figure 25, where $F(\omega)$ is the input to the system, $X(\omega)$ is the output of the system and $H(\omega)$ is the transfer function (sometimes also called as frequency response function FRF). The transfer function is the mathematical model of the system.

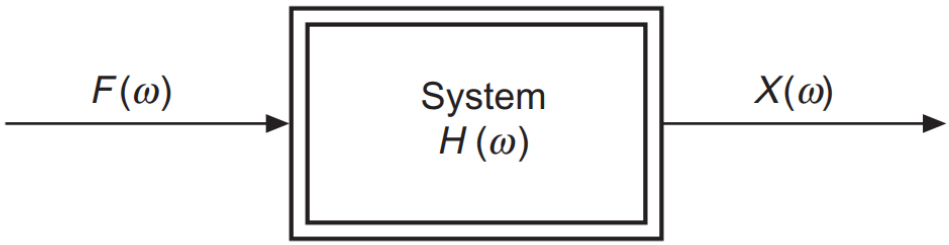

Figure 25. Single input and output system [23]

The concept shown in the Figure 25 can be presented also in the form shown in the Equation 16.

$$F(\omega)H(\omega) = X(\omega) \tag{16}$$

The Equation 16 implies that the response of the system can be calculated if the input excitation of the system is known and the proper mathematical representation of the system is formulated.

However, even if a proper mathematical model is created based on the measurements, the problem is once again the definition of the input excitation into the system in real life applications. For instance, the weight of the floating floor structures can be quite significant, quite often same order of magnitude as deck plating below it. Thus, the dynamics of the system already changes due to the variations in mass and stiffness distribution of the structure. This creates an additional modelling problem, how to solve the issue where the modelled system itself affects the input of the system.

7 Selected Approach – Finite Element Model

7.1 FE-model of the Floating Floor

The selected modelling approach was refined from the suggestions presented in the previous chapter. Because of the significant out of plane behavior in floating floor structures, using composite models or idealized plate structures did not seem to be suitable approaches. To obtain better out of plane behavior the floating floor was modelled as a composition of plate and solid elements. The deck plate and the top plate was modelled by using shell elements and mineral wool between was modelled as solid elements. The material model of mineral wool was simplified to use only basic isotropic material properties, Young's Modulus, Shear Modulus and Poisson's ratio, even though in general mineral wool slabs have different properties in different directions.

Before implementing a floating floor model into the real structure, material parameters were defined by comparing the response of a simple finite element model of a floating floor with the analytical solution of natural frequencies based on the dynamic stiffness of the resilient material.

Initially the value of Young's modulus used in the tested models was based on the value of compressive stress σ_{10}, given by Paroc Marine Floor Slab 140 datasheet, that describes how much stress needs to be applied on the mineral wool slab to obtain 10 % strain in material thickness [24]. The datasheet of the wool slab states that the compressive stress of the material used in floating floor should be more than 20 kPa. If linear behavior is assumed up to the strain of 10 %, Young's modulus of the 200 kPa is obtained from the Hooke's law $\sigma = E\epsilon$, where $\sigma = \sigma_{10}$. This value was used as a starting point for FE-model testing. Since then Paroc has removed Marine Floor Slab 140 from their catalogue, however, near equivalent materials Marine Floor Slab 130 and 150 have replaced it and have same value for compressive stress [25].

More difficult parameter to define was the damping of the mineral wool. In preliminary testing a guessed value of the critical damping coefficient of $\zeta = 5\%$ was used for the mineral wool material for the whole frequency range. Typically, in a mode-based response analysis a mode or a frequency dependent damping for whole structure is used. Therefore, the effect of damping was evaluated to see if it is worthwhile to use material damping. Using the material damping increases the complexity of analysis since the material damping cannot be defined as a function of the frequency. Therefore, mode- or frequency-based damping cannot be used for the whole structure, which is usually preferred modelling approach.

Also, as discussed earlier, the increasing model size due to the added solid and shell elements could increase the computational cost beyond acceptable level. Therefore, also the submodelling method is introduced that is capable to transfer excitations to the submodel at the adequate level.

7.2 Validation of the Material Model

Even though the model was constructed by using material and modelling parameters that were based only on good guesses, models seem to produce reasonable results when they were compared with the definition of dynamic stiffness (Equation 14) and with results of the dynamic stiffness tests, that were received from the Sika Group. The tests were

conducted on two different mineral wool slabs used in floating floor structures, Paroc Marine Floor Slab 140 and Rockwool's Marine Slab 140. In order to validate the FE-models, following two tests were carried out, comparison of natural frequencies and modelling the dynamic stiffness test setup. Comparisons are presented in the following chapters.

The test results obtained from the Sika Group are shown in the Table 1, where f_r is the resonant frequency at the zero-force amplitude, d is the sample thickness and s' is the dynamic stiffness of the sample. Tests were carried out according to EN 29052-1:1992 standard.

Table 1. Results of natural frequency and dynamic stiffness measurements obtained from Sika Group.

Material	f_r	d	s'
Rockwool Marine Slab 140	24 Hz	55 mm	5 MN/m^3
Paroc Marine Floor Slab 140	33 Hz	50 mm	9 MN/m^3

7.2.1 Comparison of Natural Frequencies

The first test was to calculate the natural frequency f_0 of the plate-wool slab-plate by using FE-model with eight different values for the Young's modulus and ten different loads and compare these results to the analytical solution (Equation 17.). The model was constructed and analyzed by using Femap 11 software with NX Nastran solver.

The model was a plate-wool-plate construction with the base dimensions of 1000 mm x 1000 mm and the total height of 66 mm. Similar construction was used as in the studied floating floor, 6 mm deck plating and 5 mm plating at the top of mineral wool layer (Figure 26). The used mesh was relatively coarse, since only out of plane modes were investigated. The structure was fixed from the bottom.

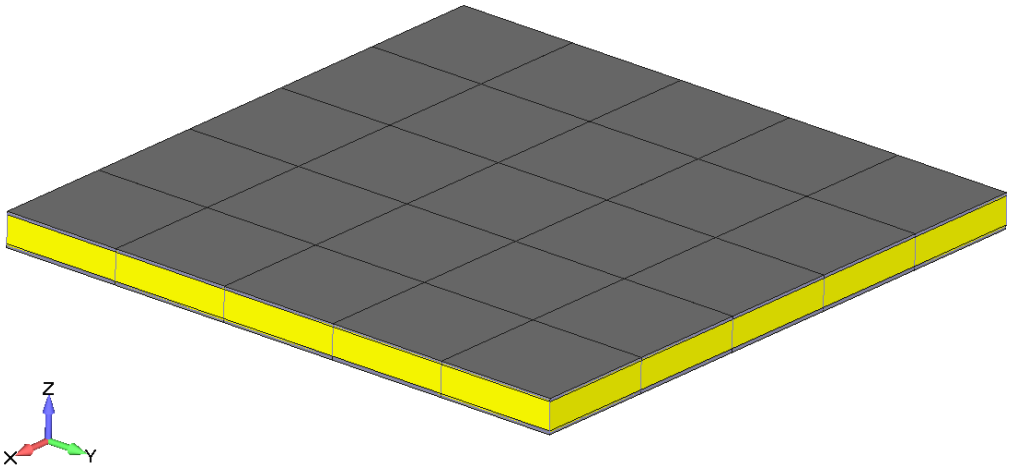

Figure 26. FE-Model for Natural Frequency Comparison

Young's modulus values and loadings used are presented in Table 2 with the results of natural frequency analysis. The smallest loading, 39.25 kg, equals to the scenario where only 5 mm thick steel plate is on the top of the resilient slab. The loading was varied by using mass elements at the nodes of the top plate.

Table 2. Model Configurations and Results of Natural Frequency Analysis

m'	E=150 kPa	E=200 kPa	E=250 kPa	E=300 kPa	E=350 kPa	E=400 kPa	E=450 kPa	E=500 kPa
kgm^{-2}	$f_0\ [Hz]$	$f_0\ [Hz]$	$f_0\ [Hz]$	$f_0\ [Hz]$	$f_0\ [Hz]$	$f_0\ [Hz]$	$f_0\ [Hz]$	$f_0\ [Hz]$
39.25	48.92	56.48	63.15	69.18	74.72	79.88	84.73	89.31
40	48.49	56.02	62.60	68.58	74.88	80.88	83.99	88.54
45	45.93	53.03	59.29	64.95	70.15	75.00	79.55	83.85
50	43.73	50.49	56.45	61.84	66.79	71.41	75.74	79.83
75	36.10	41.68	46.60	51.05	55.14	58.95	62.52	65.91
100	31.44	36.30	40.59	44.46	48.02	51.34	54.45	57.40
200	22.42	25.89	28.94	31.71	34.25	36.61	38.83	40.93
400	15.92	18.39	20.56	22.52	24.32	26.00	27.58	29.07
800	11.28	13.03	14.57	15.96	17.24	18.43	19.54	20.60
1000	10.10	11.66	13.03	14.28	15.42	16.49	17.49	18.43

The results of the analysis are presented also in Figure 27. In Figure 27 calculated natural frequency values from the FE-model are compared with the analytical solution. The comparison shows that the natural frequencies of the models with the Young's modulus of 200 kPa and 350 kPa matches quite well the analytical solution for dynamic stiffnesses of 5 MN/m^3 and 9 MN/m^3, respectively.

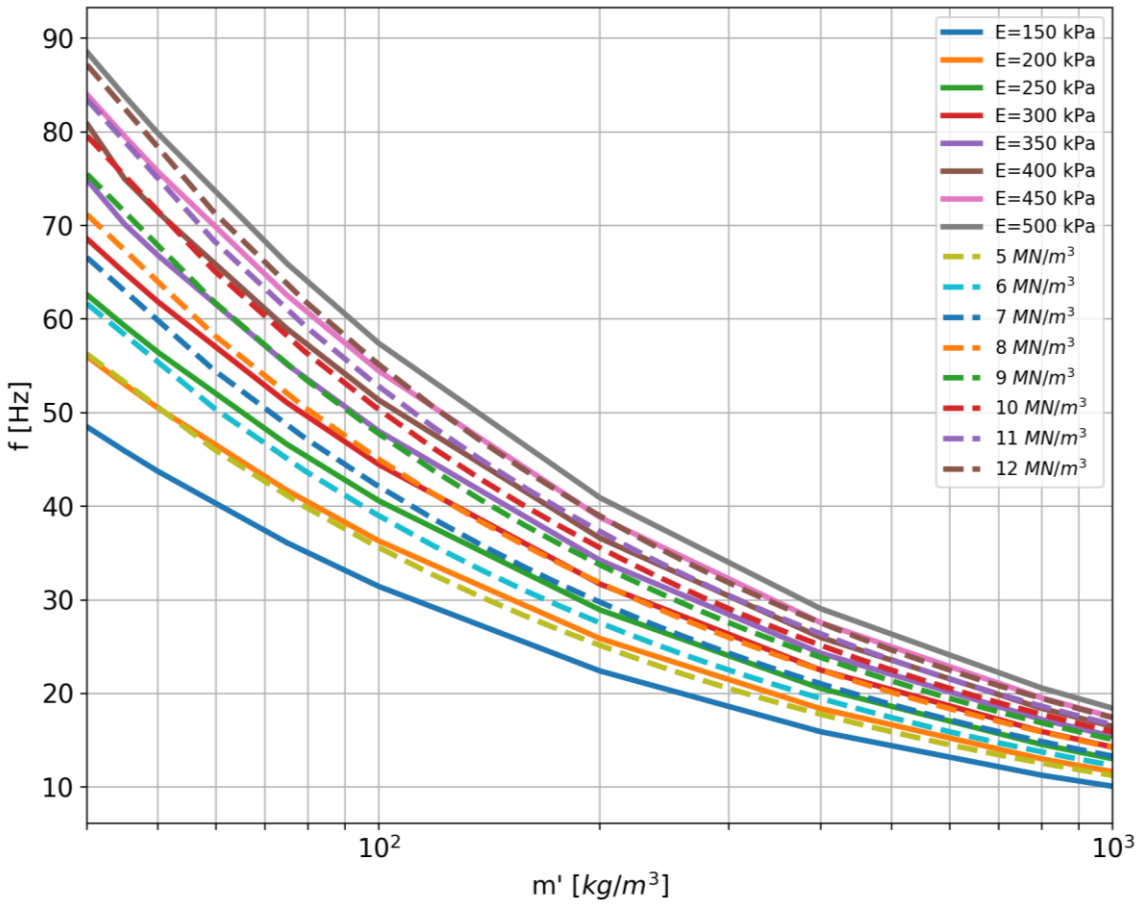

Figure 27. Results from Finite Element Analysis vs. Analytical solution. Solid lines present results from FE-simulation and dashed lines analytical solutions.

7.2.2 Modelling of Dynamic Stiffness Measurements

The second test was to replicate standardized Dynamic Stiffness – test (EN 29052-1:1992) by using FE-model and compare the results of the simulation to the actual measurement results obtained from Sika Group. The model used is presented in Figure 28. The setup is like the setup of actual measurements that were used for the comparison. The base dimensions are 200 mm x 200 mm and the thickness of the resilient slab is 50 mm. To achieve same weight of the top plate and measuring equipment (7.921 kg), approximately 25 mm thick plate elements were used. The Young's modulus of 200 kPa was used for the mineral wool material, that corresponds approximately the dynamic stiffness of 5 MN/m^3 according to tests in previous chapter. Two different values of material damping coefficient were used, $\zeta = 2$ % and $\zeta = 5$ %, to compare the effect of the damping to the response.

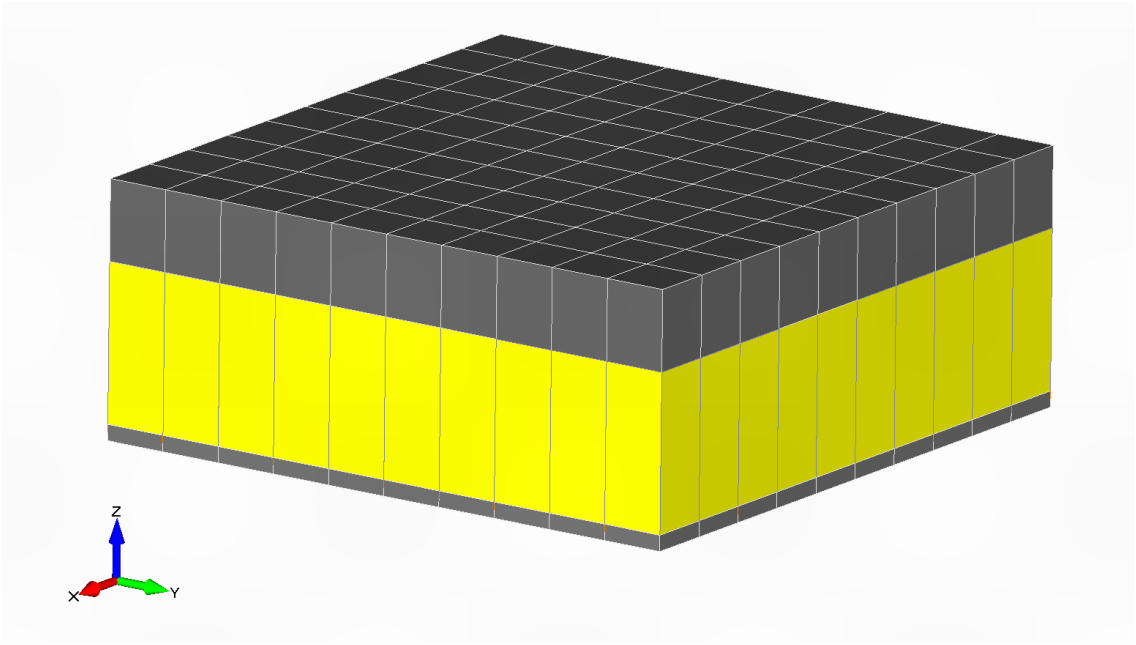

Figure 28. Dynamic stiffness measurement setup

The excitation forces of 0.2 N, 0.3 N and 0.4 N were used, and the accelerations of the top plate were extracted. The excitation force was applied at the middle of the top plate. In real experiments three different loadings were used because the measured resonant frequency changes a little bit as the excitation force changes. Hence, three different loadings were used, and the resonant frequency was extrapolated at the zero loading. That zero-loading resonant frequency was the frequency that was used to calculate the dynamic stiffness of the material.

The response amplitude and the natural frequency of the model was calculated by using forced response analysis. The analysis was conducted by using Femap 11 with NX Nastran solver. The results from the model with the Young's modulus of 200 kPa are shown in Figure 29 and Table 3. For comparison, a resonant frequency curve from the measurement report obtained from Sika Group is presented in Figure 30, where the g_n value of the measured acceleration is shown. The value of g_n is the measured acceleration divided by the gravitational acceleration.

Table 3. Results of the Dynamic Stiffness test setup simulations

		$F = 0.2\ N$	$F = 0.3\ N$	$F = 0.4\ N$
$\zeta = 2\ \%$	$A3$	$0.614\ m/s^2$	$0.921\ m/s^2$	$1.228\ m/s^2$
	f_r	$25.9\ Hz$	$25.9\ Hz$	$25.9\ Hz$
$\zeta = 5\ \%$	$A3$	$0.248\ m/s^2$	$0.371\ m/s^2$	$0.495\ m/s^2$
	f_r	$26.1\ Hz$	50.49	56.45

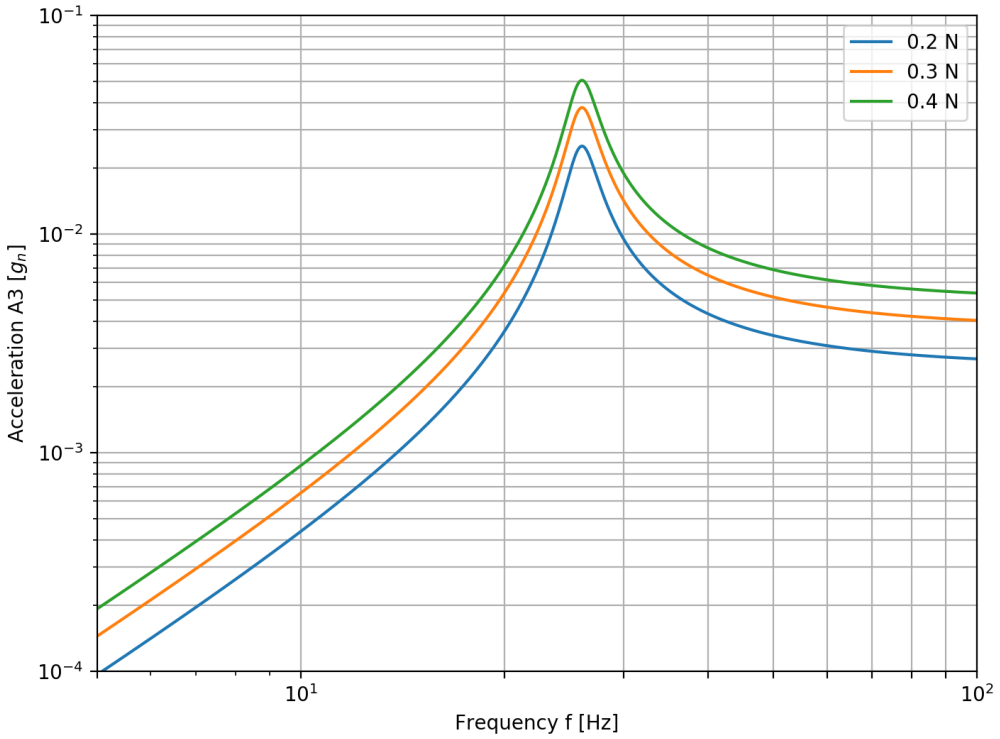

Figure 29. Response of Dynamic Stiffness - simulation. E=200 kPa and ζ=5 %

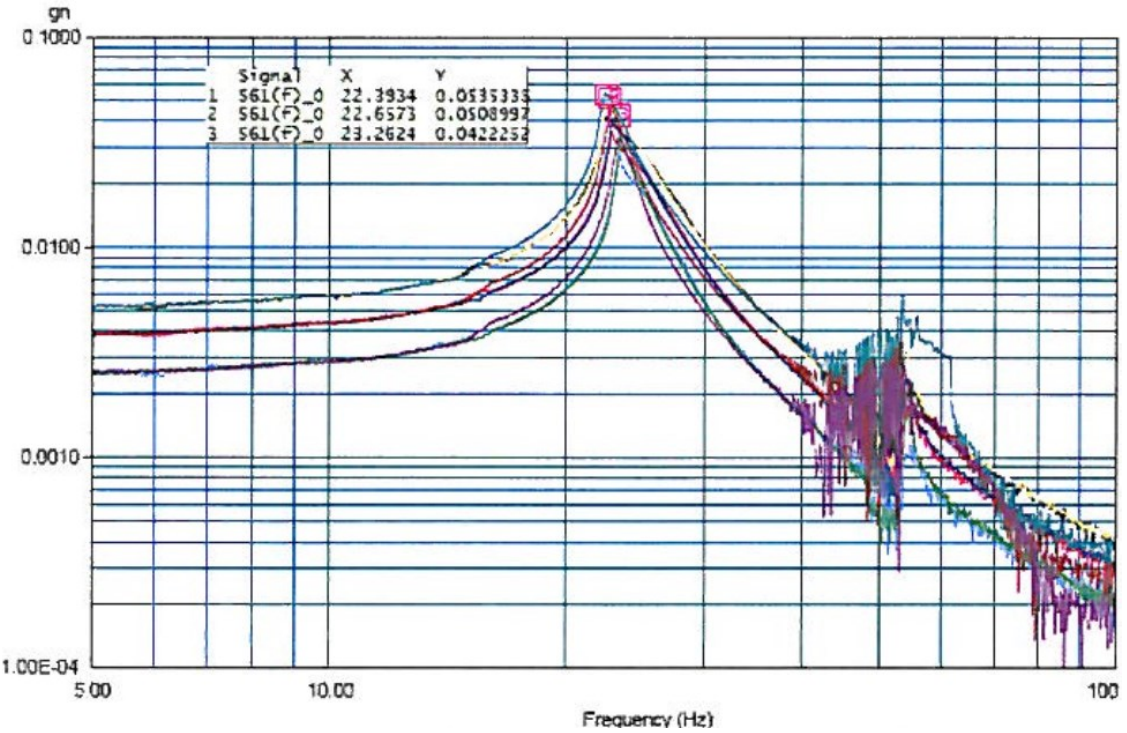

Figure 30. Resonant frequency curves of a Rockwool Marine Slab 140 test piece from the measurement report obtained from the Sika Group.

The comparison of the results shows that the magnitude of the response is same in both, FE-model and actual measurements. Very detailed comparison is difficult because there is plenty of variation in measured accelerations.

In Figure 31 the response of dynamic stiffness simulation with the critical damping coefficient of $\zeta = 2\%$ is presented.

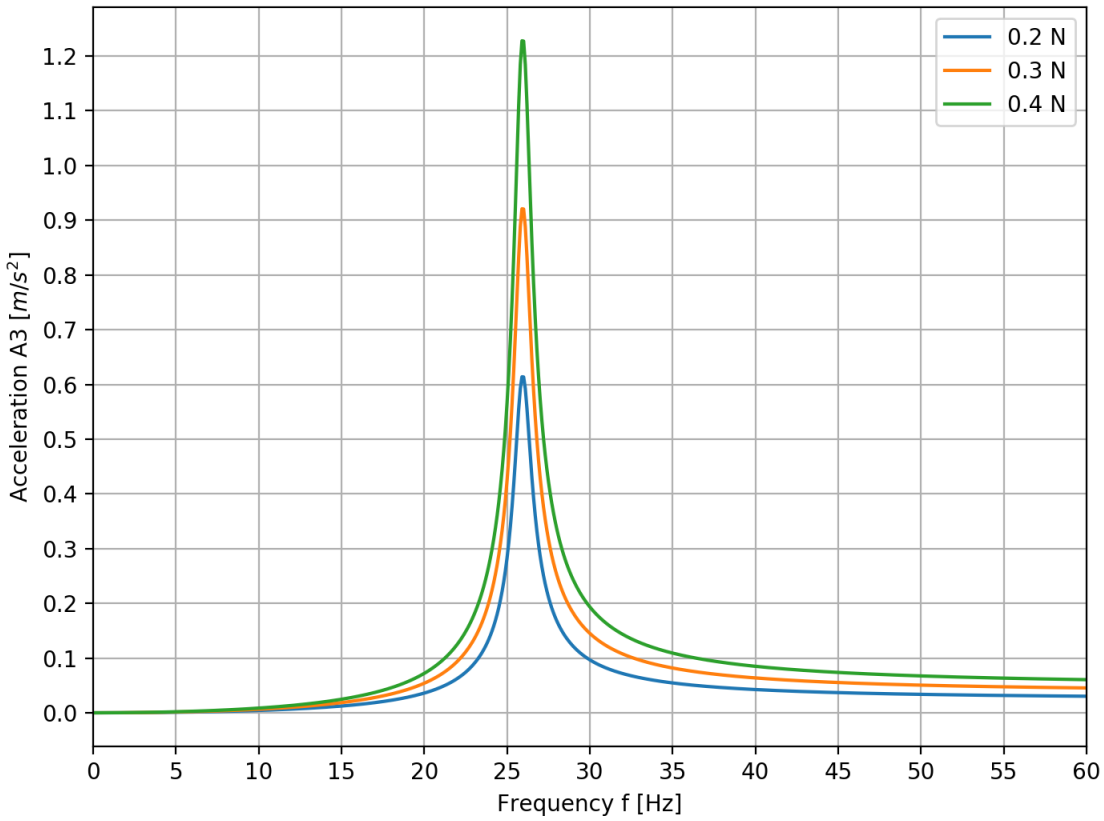

Figure 31. Response of Dynamic Stiffness - simulation. E=200 kPa and ζ=2 %

The comparison between responses in Figure 32 shows that increasing the critical damping coefficient from 2 % to 5 % decreases the vibration amplitude by 59.3 %, from 1.23 m/s^2 to 0.50 m/s^2 when 0.4 N excitation force was used. The effect of the damping might seem quite large, however, the magnitudes of the responses are still at the same level. In general, when measured vibration amplitudes in ships are compared to the calculated vibration amplitudes, a factor of three is not uncommon difference level [4]. Since the difference between vibration magnitudes is reasonable, the same 2 % damping can be used for mineral wool as used for the ship structure in general.

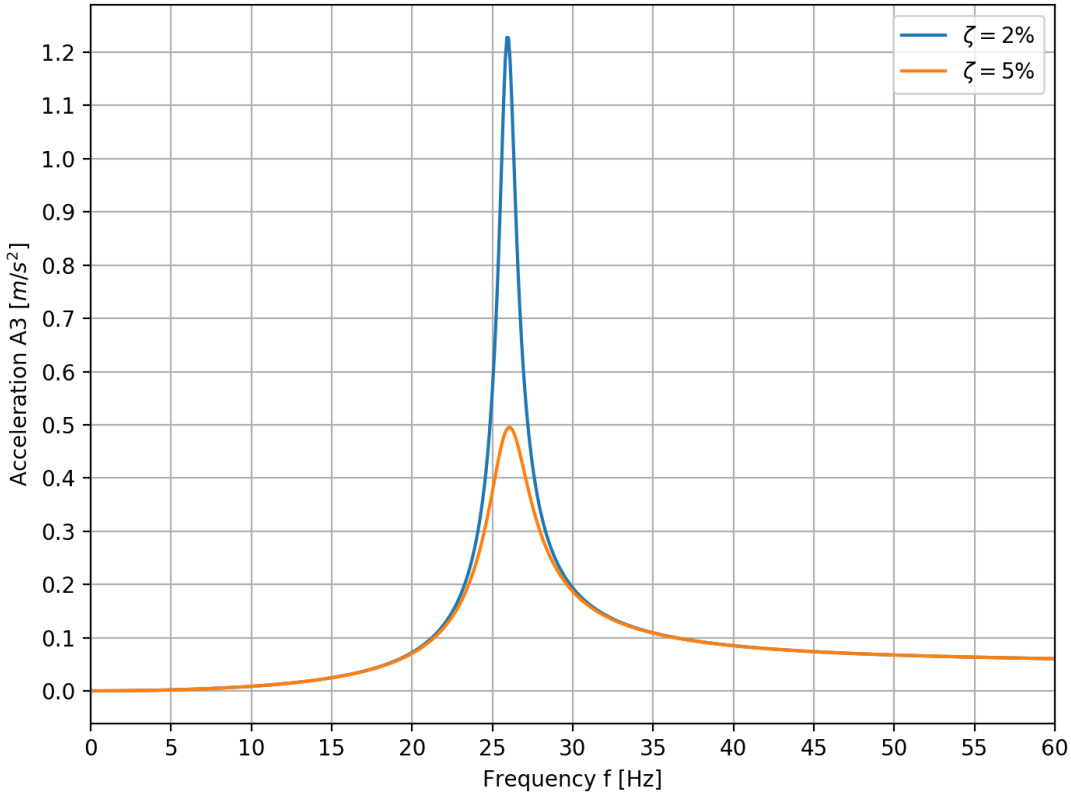

Figure 32. Effect of the damping to the amplitude of the acceleration with the applied 0.4 N excitation force.

7.3 Submodelling Procedure

The submodelling procedure was created and tested using the Finite Element Model of the NB 512 ship (Figure 33), one of the sister ships of NB 511. In the submodelling procedure the response of global model was solved by using direct frequency response analysis in Femap 11 with NX Nastran solver and the results were used as an input to the submodel of the area of interest (Figure 34).

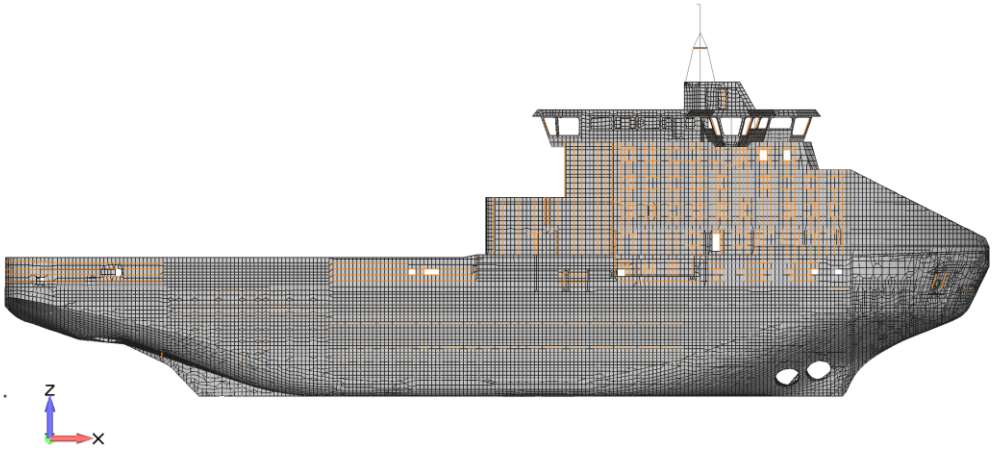

Figure 33. Global model of the NB 512 ship

In the forced response analysis of the global model, following exciting forces from the propulsion system and from the machinery were applied simultaneously:

- Excitation forces from Azipods – Total of 8 kN (2 x 4 kN) in vertical direction. Both propulsion units in same phase
- Main engine excitations – Total of 10 kN vertical force applied on engine bedding.

Responses were calculated between 10 and 20 Hz with 0.5 Hz increments. Global structural damping equivalent to critical damping coefficient $\zeta = 2\ \%$ was used for whole frequency range.

The submodel was created by copying all nodes and elements from the area of interest in the global model to the new empty model. The numbering of nodes and elements was kept as in the global model since the submodelling method used operates in node-to-node basis i.e. output of the node N in the global model will be transferred into the input to the node N in the submodel. At least in Femap this is quite quick and straightforward way to create a submodel.

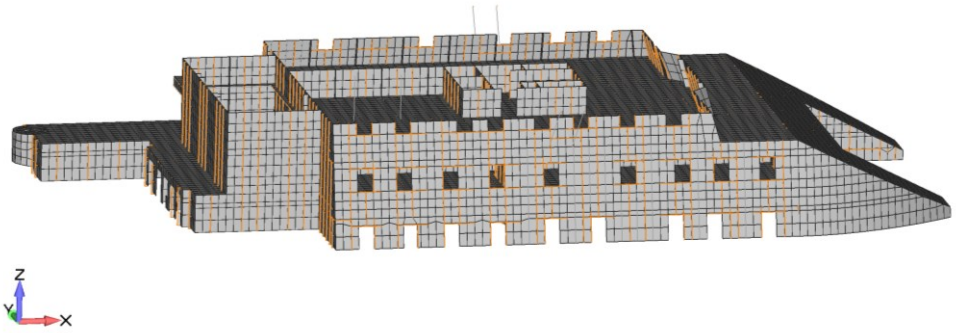

Figure 34. Submodel of 2nd bridge deck and its surroundings.

Since Femap does not have a feature that allows to transfer frequency dependent loads between models, some custom tools had to be created. The output data from the global model i.e. X-, Y- and Z-accelerations and corresponding phase information, was extracted to the CSV-file. The data was extracted from the nodes at the interface between the global and the submodel regions (Figure 35).

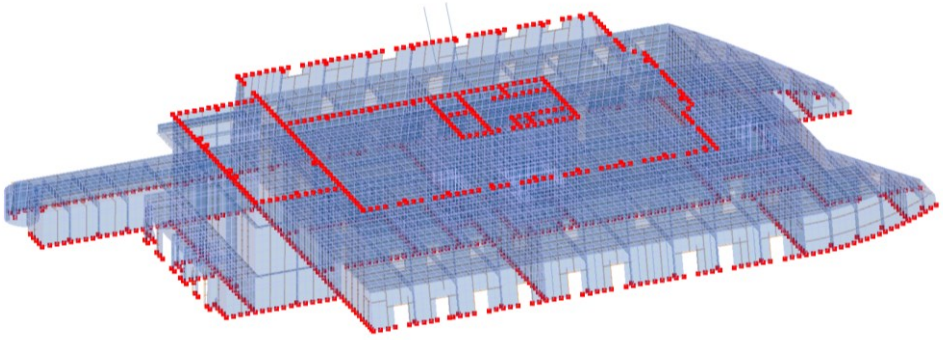

Figure 35. Nodes at the interface between the global and the submodel highlighted red

The load transfer process was divided into two parts, preprocessing the data from the global model and reading the input data to the submodel. The main idea was to create a Femap API-script that reads input values for each node from the corresponding txt-files. Because of this approach, a Python script was created to preprocess output data from the global model such way that accelerations and corresponding phases are stored in individual txt-files for each node. Basically, the whole load transfer process could have been carried out by using a single Femap API-script, however, using different scripts makes it possible to use some other methods to create frequency dependent nodal input data in future applications if needed. The load transfer process is shown in Figure 36.

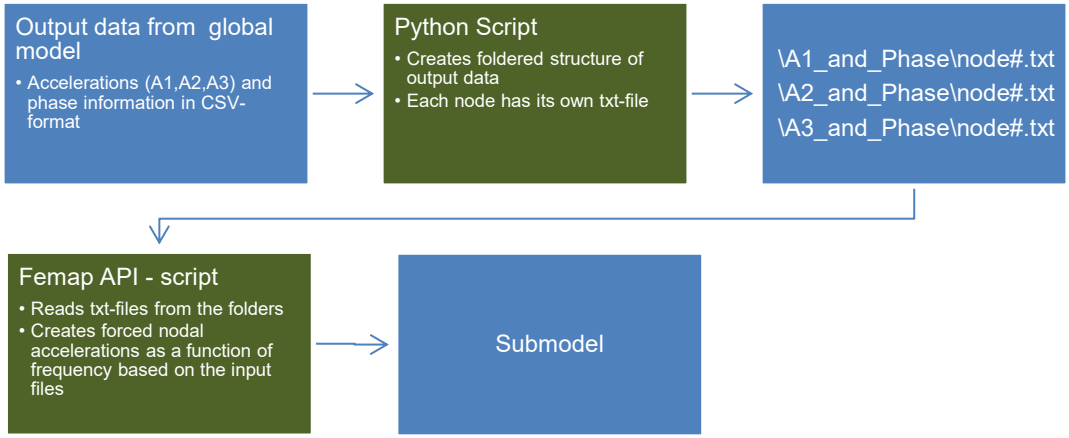

Figure 36. Flowchart of the load transfer process between the global and the submodel

The created submodelling procedure was tested by comparing the results of the global analysis with the results from the submodel. In Figure 37 results of the global model analysis are shown. In Figure 37 the maximum values of vertical velocities at the 2nd bridge are shown.

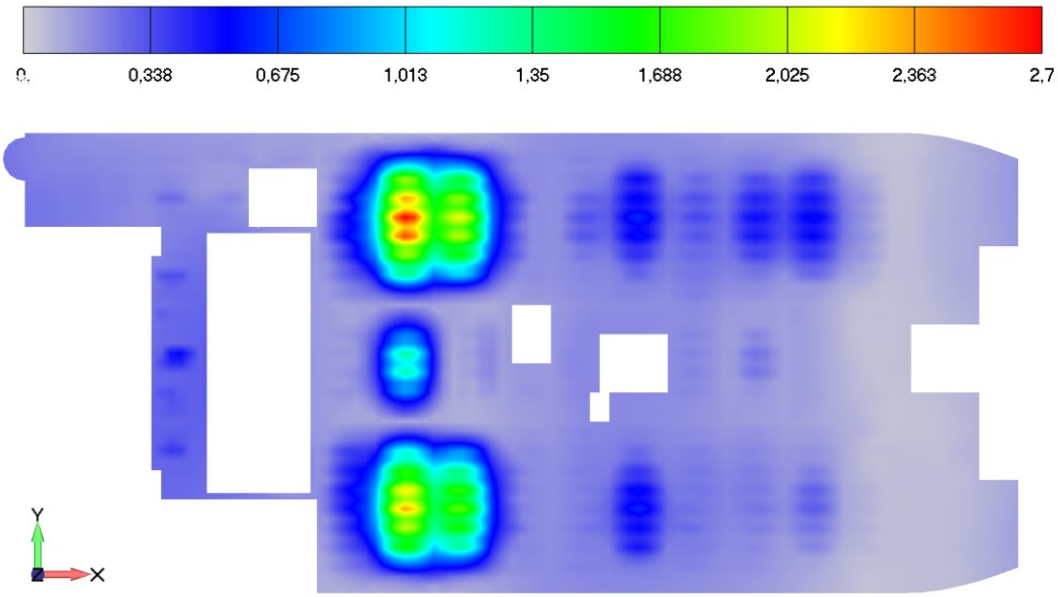

Figure 37. Global model - Maximum vertical velocities (mm/s) at the 2nd bridge deck. Maximum values at whole frequency range of 10-20 Hz.

In Figure 38 the maximum values of vertical velocities from the submodel are shown at the same location. When Figure 37 and Figure 38 are compared, it can be immediately seen that the submodelling method seems to work well. For the most part, velocity contours seem similar, only at the one location some visible increase in vibration velocities can be seen.

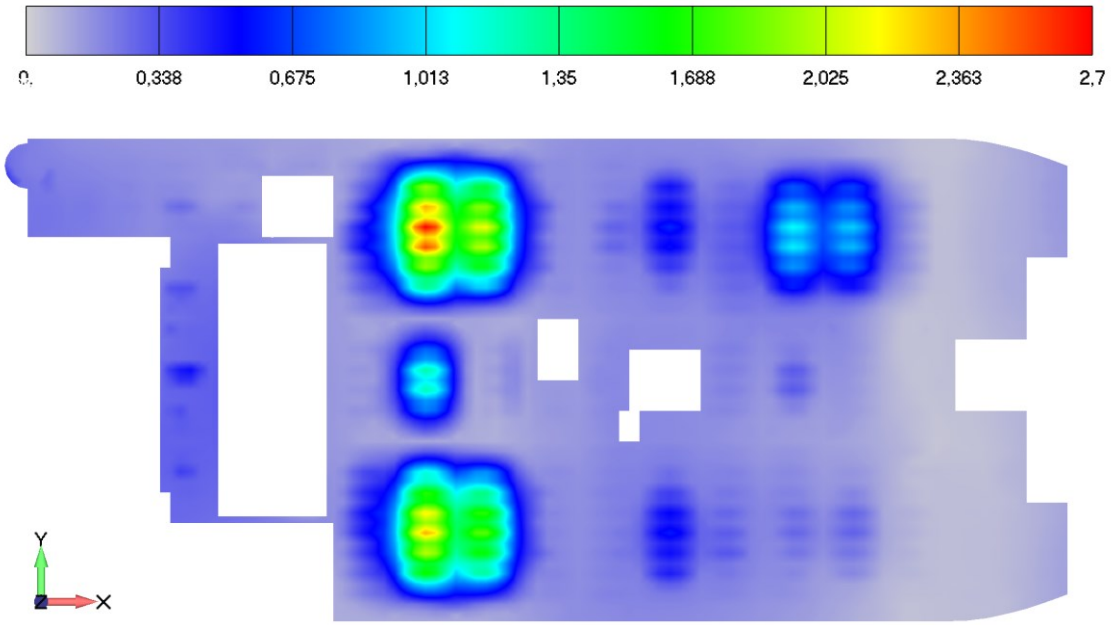

Figure 38. Submodel - Maximum vertical velocities (mm/s) at the 2nd bridge deck. Maximum values at whole frequency range of 10-20 Hz.

In Figure 39 the relative difference in velocities between models is visualized. Like seen in the previous Figures, at one area significant increase in velocities occur.

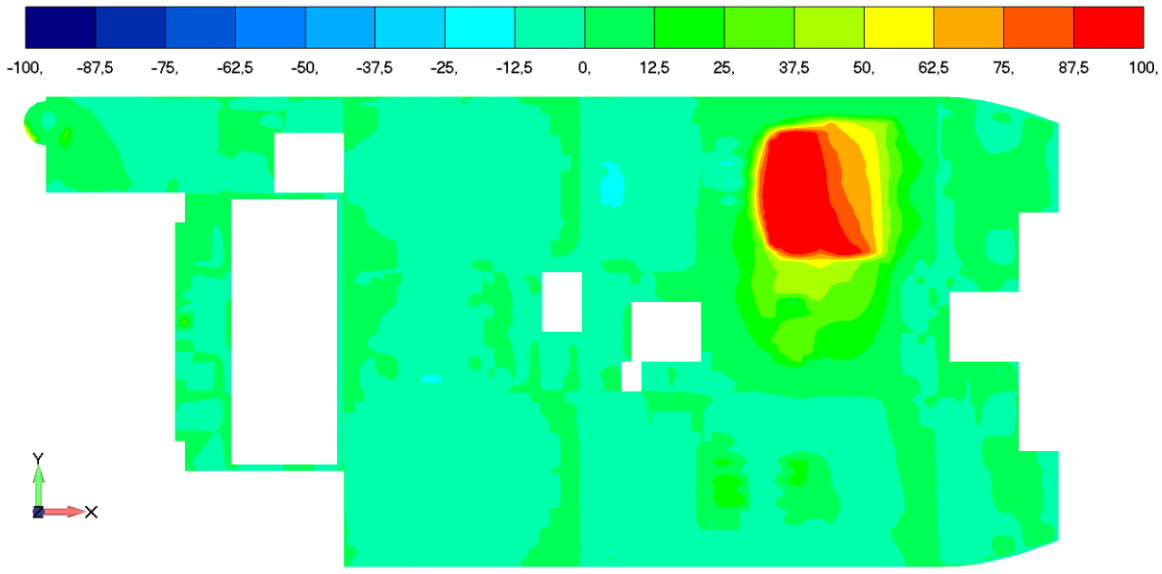

Figure 39. Visualized relative difference between the results of the Submodel and the Global model. The contour is set from -100 % to 100 %.

At this location, the maximum difference to the global model was +157 %, which seems at first to be a quite large increase, however, when absolute values are compared, the situation seems to be more reasonable. For instance, in this node where the 157 % increase occurs, the absolute increase was only 0.36 mm/s, from 0.23 mm/s to 0.59 mm/s. Based on this comparison, it can be stated that the used submodelling procedure produces reasonable results and it can be used for the further analysis.

8 Case Study – Vibration Analysis of a Ship

In this case study, the model of the floating floor was applied to the finite element model of the NB 511 ship and the functionality of the modelling method was investigated. The floating floor model was implemented into the submodel of the 2nd Bridge Deck that was one of the locations where vibration problems have occurred in the past. The global finite element model used was the same model that was used for strength and vibration analysis during the design process of the NB 511 ship. The model of the NB 511 was used since there was some amount of reports, data and measurements available on occurred vibration problems.

The case study chapter has the following structure. At first, used finite element model is introduced. Next, forced vibration analysis will be applied on the global model and the acceleration responses will be extracted at the interface of the submodel of the local structure. The response of the submodel will be analyzed by using the forced response analysis and the functionality of the submodel will be validated by comparing the results with the global model. The mesh of the submodel will be refined by halving the average element size and the results are compared once again to the global model.

When the functioning submodel is achieved, the floating floor model will be implemented into the model and different loading scenarios will be created. The forced response analysis will be applied with different loading cases and configurations and the response will be studied.

8.1 Finite Element Model of the Ship

The used model of the ship NB 511 was the same model as used in FE-analysis of the ship during the design process. The model was constructed by using shell, beam and mass elements. The average element size of shell elements used was approximately $400\ mm \times 400\ mm$. The finite element model of the ship is shown in Figure 40.

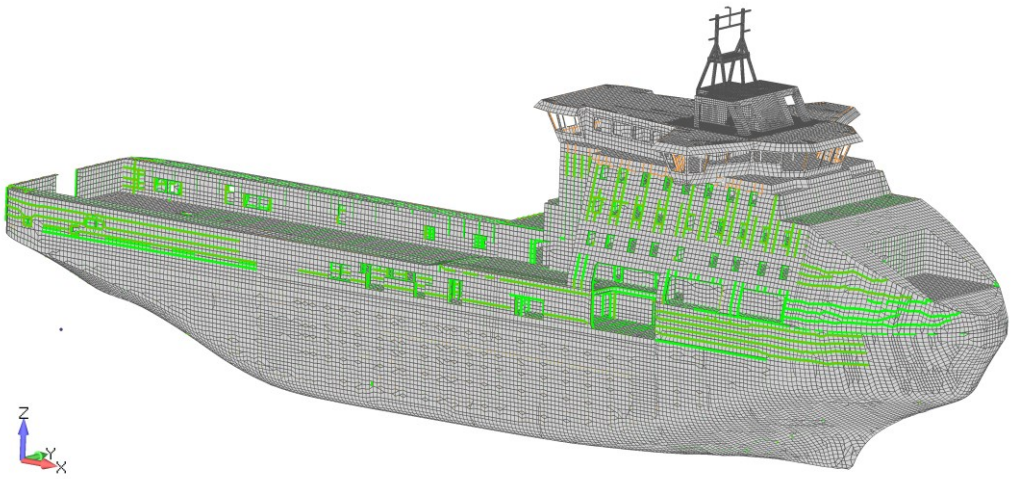

Figure 40. FE-model of the NB 511 ship. Plate elements visualized in grey and beam elements in green.

Basic material properties of AH36 steel was used, Young's modulus of 206 GPa and Poisson's ratio of 0.3. The density of the material was scaled to take into account for instance the outfitting masses, masses from the main equipment and weight of the cargo.

Therefore, for most of the structure the material density of 13200 kg/m^3 was used. Also, the mass of the surrounding water was taken into account. The surrounding water mass was calculated to be 10130 tons and the mass was distributed on the ship's hull below the design draught of 7600 mm, by using mass elements. The mass of the ships structure was 9167 tons, thus the total mass of the model was 19297 tons.

8.2 Vibration Analysis of the Global Model

In the vibration analysis, the frequency range from 10 Hz to 16.5 Hz was considered. The response of the system was calculated by using 0.5 Hz increments at the frequency range. The used frequency range covers excitation frequencies from the Azipod propulsion units and from main engines with the 10% frequency band around nominal excitation frequencies. Excitation frequencies are presented in Table 4.

Table 4. Excitation sources and frequencies

Excitation Source	Nominal Excitation Frequency	Frequency Band of 10 %
Azipod (Bollard)	11.1 Hz	10.0 Hz – 12.2 Hz
Azipod (Open Water)	15 Hz	13.5 Hz – 16.5 Hz
Main Engines	12.5 Hz	11.3 Hz – 13.8 Hz

The global vibration analysis was carried out by using five different load cases. Used load cases are shown in Table 5. Only vertical excitation forces were applied in load cases. Same values for the Azipod and main engine excitations were used as in the vibration analysis done during the design of the ship. Used values were provided by the component suppliers.

Table 5. Load Cases used in the Vibration Analysis of the Global Model

Load Case	Azipod Port F_z	Azipod Starboard F_z	Main Engines F_z
LC1	3950 N	3950 N	0 N
LC2	3950 N	-3950 N	0 N
LC3	3950 N	3950 N	21000 N (70 %)
LC4	0 N	0 N	21000 N (70 %)
LC5	0 N	0 N	5000 N (1/6)

Load cases LC1 and LC2 include only excitations from both Azipod propulsion units. In LC1, the excitation forces are in the same phase and in the LC2 excitation forces are in the opposite phases. In the case of main engines, the vertical foundation excitation force

of 5 kN was used for each main engine, thus the theoretical maximum vertical peak excitation from the main engines was 30 kN. However, to achieve maximum excitation forces all the engines should operate at the same phase, which is not very realistic. Nevertheless, in LC3 and LC4 rather arbitrary 70 % of the maximum theoretical peak excitation force was used. The last load case, LC5 includes only vertical excitations from one main engine.

In the analysis, overall structural damping coefficient $G = 4\ \%$ was applied for the whole frequency range. At the resonant frequencies $G = 4\ \%$ is equivalent to the critical damping of $\zeta = 2\ \%$. Because the structural damping coefficient affects the stiffness of the structure, the damping forces are constant through the frequency range, unlike in the case of viscous damping where the damping forces increase when the forcing frequency increases [11]. The chosen damping was loosely based on the Lloyd's Register guidance notes [7]. Damping values used by Lloyd's Register are shown in Table 6.

Table 6. Damping at the different frequency ranges according to Lloyd's Register

Frequency	Critical Damping ζ	Structural damping $G = 2\zeta$
0-5 Hz	1 %	2 %
5-20 Hz	1-3 % (linear increase)	2-6 % (linear increase)
>20 Hz	3 %	6 %

In Figure 41 the results of the vibration analysis of load cases LC1 and LC2 are shown. It can be seen that due to the excitations only from Azipods, excessive vibrations do not occur in the studied area of 2nd bridge deck.

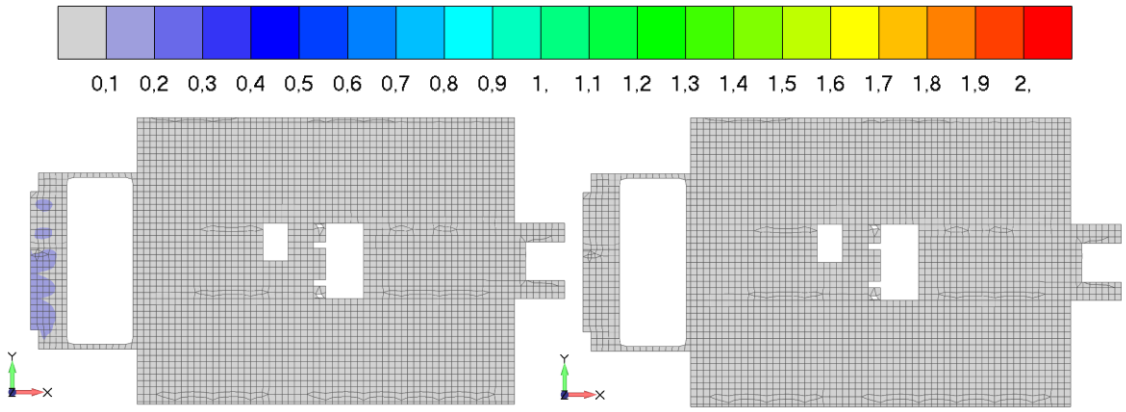

Figure 41. LC1 (left) and LC2 (right) maximum vertical vibration velocities (mm/s) at the frequency range of 10-16.5 Hz.

The results from the load cases LC3 and LC4 are shown in Figure 42. In these results some noticeable amount of vibrations occurs. Even though the magnitude of main engine vibration excitation used are approximately three times higher than the excitations from

the Azipods, yet it can be deduced from these results that the main engines contributes more on vibration generation in the studied location than Azipods.

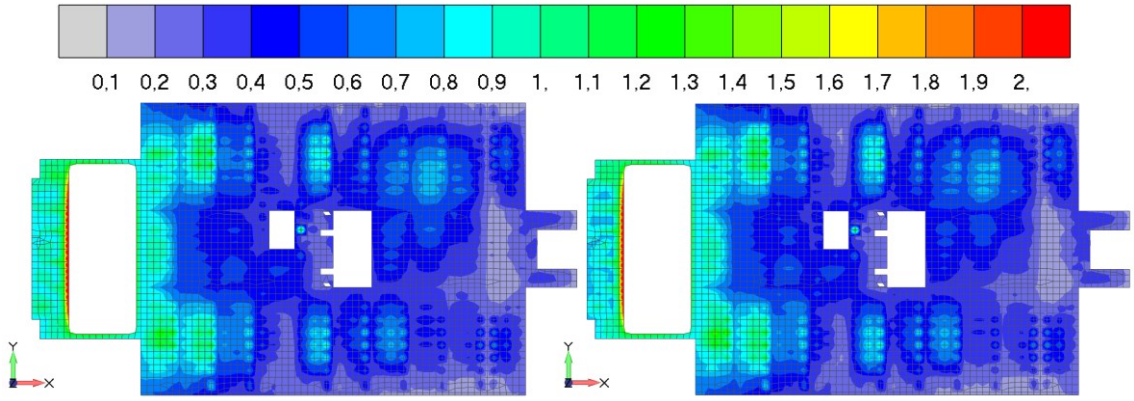

Figure 42. LC3 (left) and LC4 (right) maximum vertical vibration velocities (mm/s) at the frequency range of 10-16.5 Hz.

In Figure 43 the results from LC5 are shown where the ship structure is excited only by one main engine with the 5 kN vertical force. These results confirm the deduction mentioned before, that the main engine contributes more in vibration generation in the studied location. This is understandable since the propulsion units are located reasonable far from the 2nd bridge deck (Deck 7), when the main engines are located a few decks below the studied area on the Deck 3.

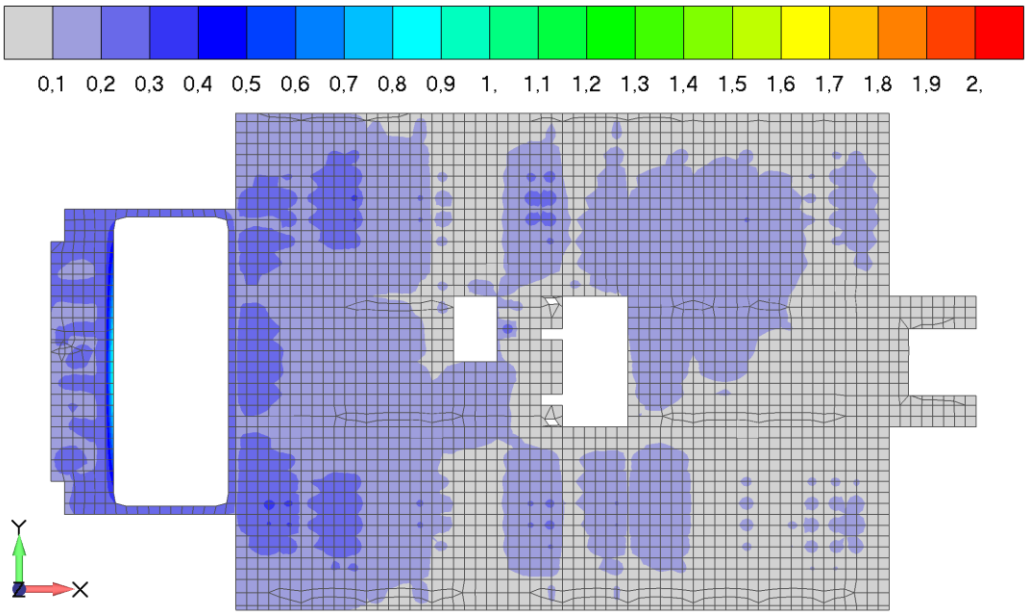

Figure 43. LC5 maximum vertical vibration velocities (mm/s) at the frequency range of 10-16.5 Hz.

8.3 Submodel of Local Structure

The submodel of the 2nd Bridge Deck shown in Figure 44 was created in the same manner as described in Chapter 7.3. In Figure 45 a cutout view of the submodel structure is shown, where inside structures like walls can be seen. The load case LC3 was used in the vibration analysis of the submodel since it includes excitation from the both main excitation sources, from the propulsion system and from main engines.

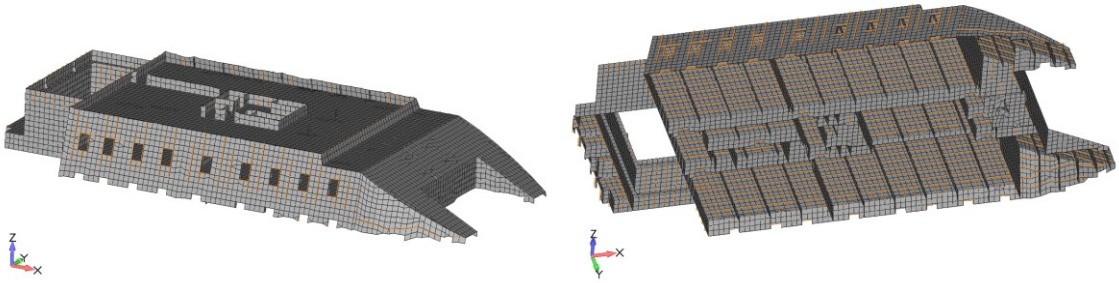

Figure 44. Submodel of the 2nd Bridge Deck

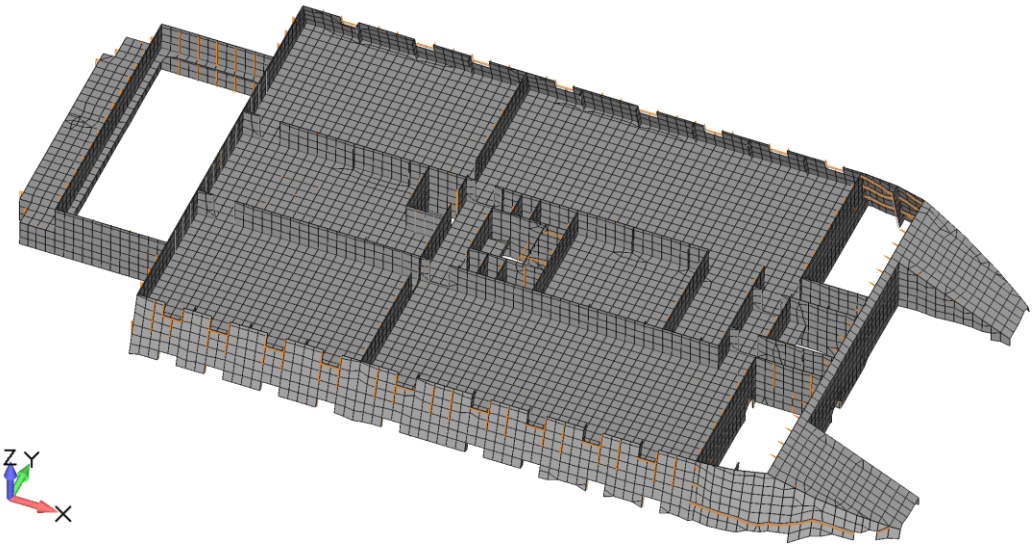

Figure 45. Cutout view of the submodel

At first, the submodel was created and the responses from the global model analysis in the previous chapter was used as excitations. Exciting accelerations were applied on the nodes at the bottom and top boundaries of the submodel. Same material and damping parameters were used as in the global vibration analysis.

The calculated vertical velocities of the 2nd bridge deck floor were compared with the global vibration analysis results. Also, the refined FE-model was analyzed where the finite element mesh of the submodel was refined by 2:1 ratio. The average elements size

of the refined submodel was approximately 200 mm x 200 mm. The results of the vibration analysis of the both submodels, non-refined and refined, are shown in Figure 46 where the maximum vertical velocities of the floor are shown at the frequency range of 10 Hz to 16.5 Hz. The same 0.5 Hz increment was used in the analysis as in the global model analysis.

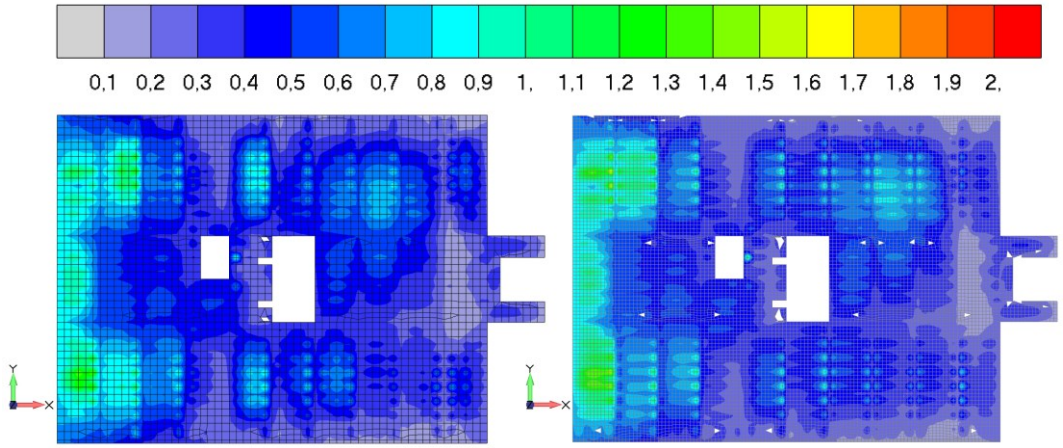

Figure 46. Vertical velocities (mm/s) of the 2nd Bridge Deck. Non-refined model (left) and refined model (right)

When the results of the analyzed submodels (Figure 46) are compared with the results of the global model (Figure 42), the functionality of the submodels can be verified since there are no significant differences between the results. The refinement of the mesh creates nodes where excitations are not applied, still the results seems to match the results from the global model. Therefore, these models can be used in the further investigations of the floating floor model.

8.4 Investigation of Floating Floor Model

8.4.1 Finite Element Model

The submodels of the 2nd Bridge Deck tested in the previous chapter were utilized in this section. However, a few small changes were made. In the global analysis and in the submodels used in the previous chapter, the density of the steel material was scaled up to take into the account the outfitting masses and other masses with the distributed nature. However, since the floating floor structure was implemented into the submodel, the general material density of 7850 kg/m^3 for steel was used in these models. In the local scale this corresponds better the mass distribution of the real structure, since the floating floor structure adds some mass where it is applied. The excitations were applied by using the smaller frequency increment of 0.1 Hz, therefore the global model had to be reanalyzed.

The implementation of the floating floor model was quite straightforward. At the area where the floating floor was used in the ship (Figure 47), the shell elements were copied and transferred upwards by 50 mm i.e. is the thickness of mineral wool slabs used in the floating floor. After that, the matching layer of the solid elements were created between the two layers of shell elements and the material properties of the mineral wool were assigned on these solid elements. The used material properties were based on the studies presented in Chapter 7.

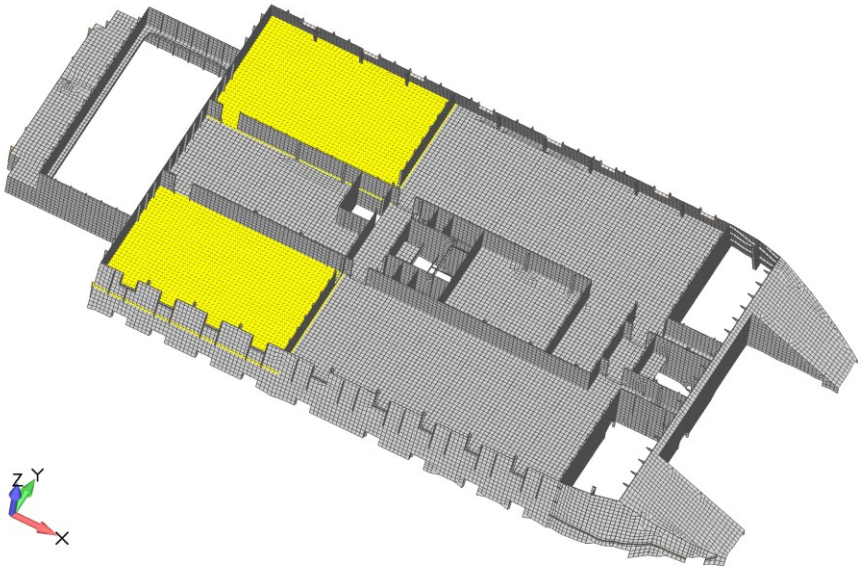

Figure 47. The area where the floating floor model was implemented highlighted yellow

The modelled floating floor structure is presented in Figure 48 where some of the surrounding structures are also visible. Material thicknesses and beam profiles are also visualized in Figure 48.

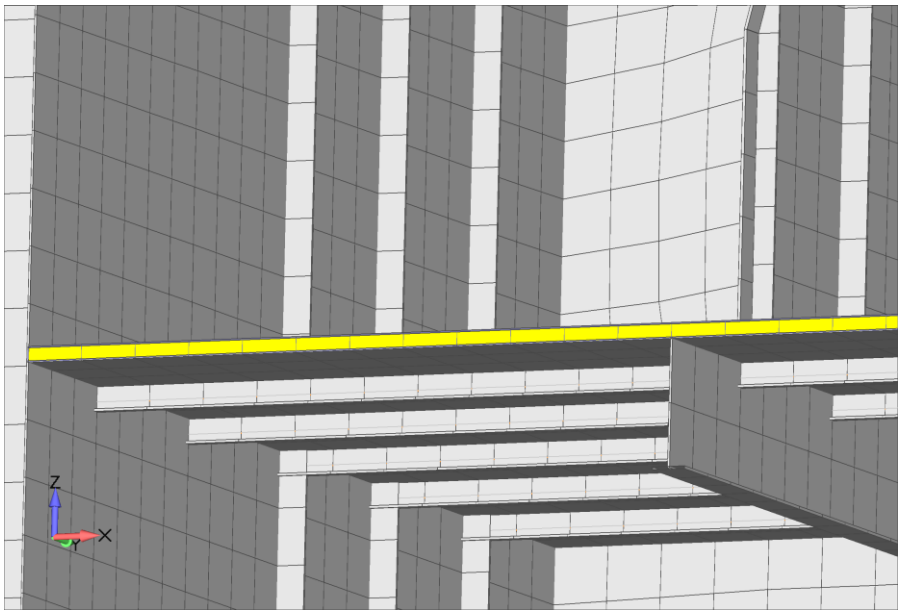

Figure 48. Implemented floating floor structure in a model.

The response of the floating floor structure was analyzed by using different loading conditions for the floating floor and all analyzed models used the submodel with the refined mesh. Used material properties are presented in Table 7 and studied loading conditions are listed below. The applied excitation was retrieved from the analysis of the global model by using the load case LC3, where Azipods provided in total of 7900 N vertical exciting force and main engines 21 000 N vertical exciting force. The response of the studied structure was solved between 10 Hz and 16.5 Hz by using 0.1 Hz frequency increments.

Studied Load Cases:

- LC3a – Steel deck only - no applied floating floor
- LC3b – Steel deck only with cabin masses ≈ 360 kgm^{-2}
- LC3c – Floating Floor without additional loading
- LC3d – Floating Floor with cabin loads ≈ 160 kgm^{-2}
- LC3e – Floating Floor with cabin loads ≈ 360 kgm^{-2}

Table 7. Material properties used in FE-model.

Material	Young's Modulus E $[MPa]$	Poisson's ratio ν	Density ρ $[kg/m^3]$	Dynamic Stiffness s' $[MN/m^3]$	Yield Strength $[MPa]$
AH36 Steel	206 000	0.3	7850	-	355
Rockwool Marine Slab 140	0.2	0.3	140	5	-

In the models where cabin loads were used, the weight of cabin modules were applied as non-structural mass properties along the edges of the cabins as well as at the areas where the wet units were located in cabins (Figure 49). The weight of each cabin was assumed to be roughly 1600 kg and the studied accommodation area contains in total of 7 cabin units. Therefore, the total applied weight was approximately 11 200 kg. The area where the weight of the cabins was distributed was around 31 m^2, thus the load of 360 kgm^{-2} was used as normal condition. The floating floor was also analyzed without loading and by using the load of 160 kgm^{-2}. The load of 160 kgm^{-2} was chosen to get some results between unloaded and loaded conditions.

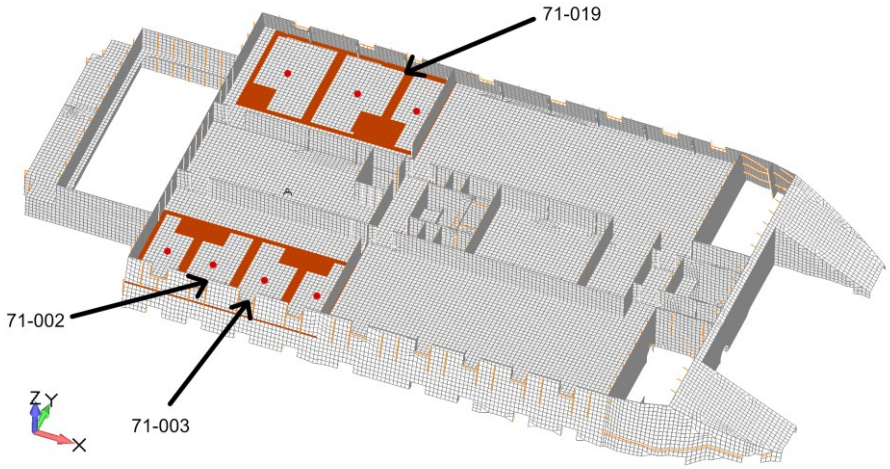

Figure 49. The area of applied cabin loads highlighted red. Measurement nodes marked as red dots.

8.4.2 Results of the Analysis

A few aspects were considered when the results of the analyzed load cases were processed. Firstly, maximum velocities were visualized for the comparison of vibration levels in general. This provides a good basis for the further investigations where the results from the measurement nodes (Figure 49) are compared. The maximum velocities of bare deck load cases LC3a and LC3b are presented in Figure 50 and in Figure 51 the maximum velocities of LC3c where the floating floor was implemented without cabin masses.

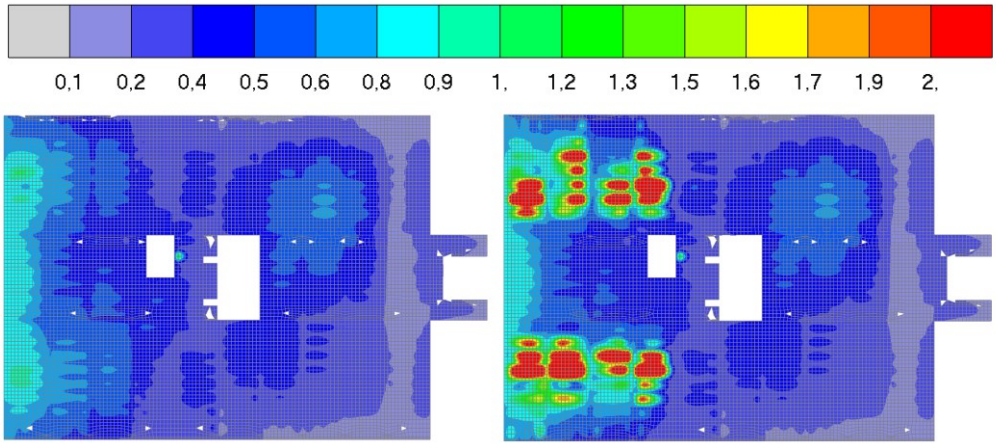

Figure 50. LC3a and LC3b maximum vertical vibration velocities (mm/s) at the frequency range of 10-16.5 Hz

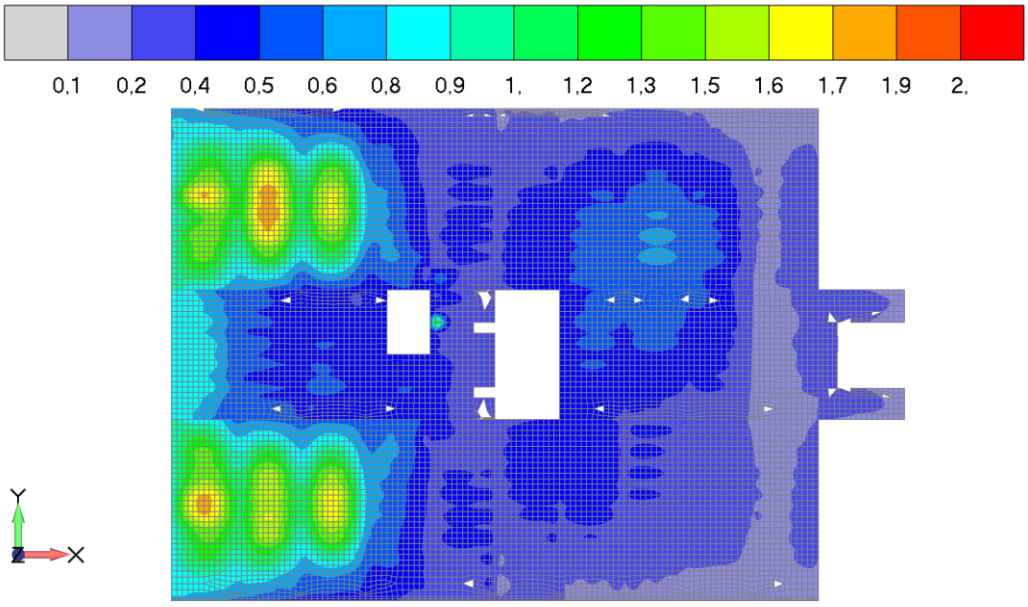

Figure 51. LC3c maximum vertical vibration velocities (mm/s) at the frequency range of 10-16.5 Hz

In Figure 52 the maximum vertical vibration velocities of load cases LC3d and LC3e are shown. From these figures it can be seen, that the applying the cabin loads increases local vibration levels quite significantly. The comparison of Figure 51 and Figure 52 shows that the increasing the localized masses also concentrates vibration peaks to the smaller areas. Especially in load cases LC3d and LC3e very high velocity peaks (around 15 mm/s)

occur at the locations where cabin masses are applied. However, elsewhere the velocity profile seems quite reasonable.

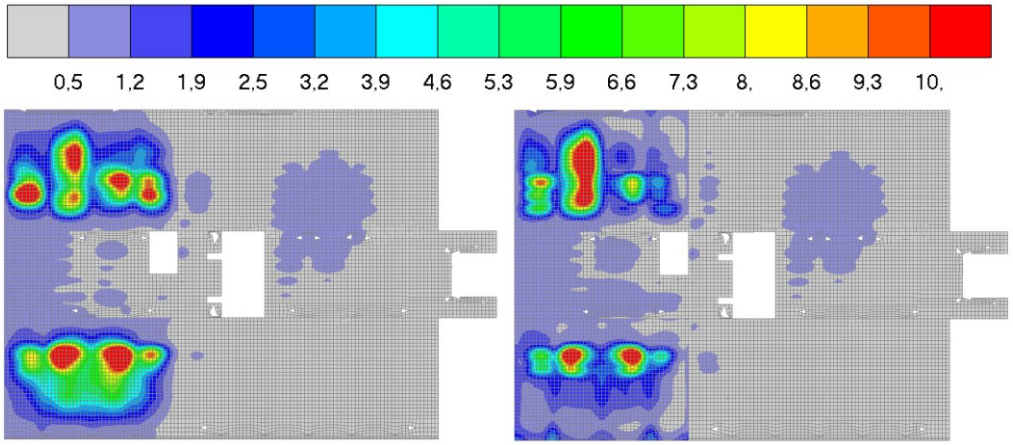

Figure 52. LC3d and LC3e maximum vertical vibration velocities (mm/s) at the frequency range of 10-16.5 Hz

The focus was on cabins where vibration problems had occurred in the past i.e. cabins 71-002, 71-003 and 71-019. Vertical velocities were measured from the locations roughly middle of the cabins and the results between load cases were compared. Locations of measurement nodes are shown in Figure 49.

Vertical velocities from the measurement nodes of cabins 71-002 and 71-003 are presented in Figure 53 and Figure 54, respectively. Somewhat surprisingly a significant peak in the vibration velocity occurs in load case LC3d where 160 kgm^{-2} cabin loads are applied.

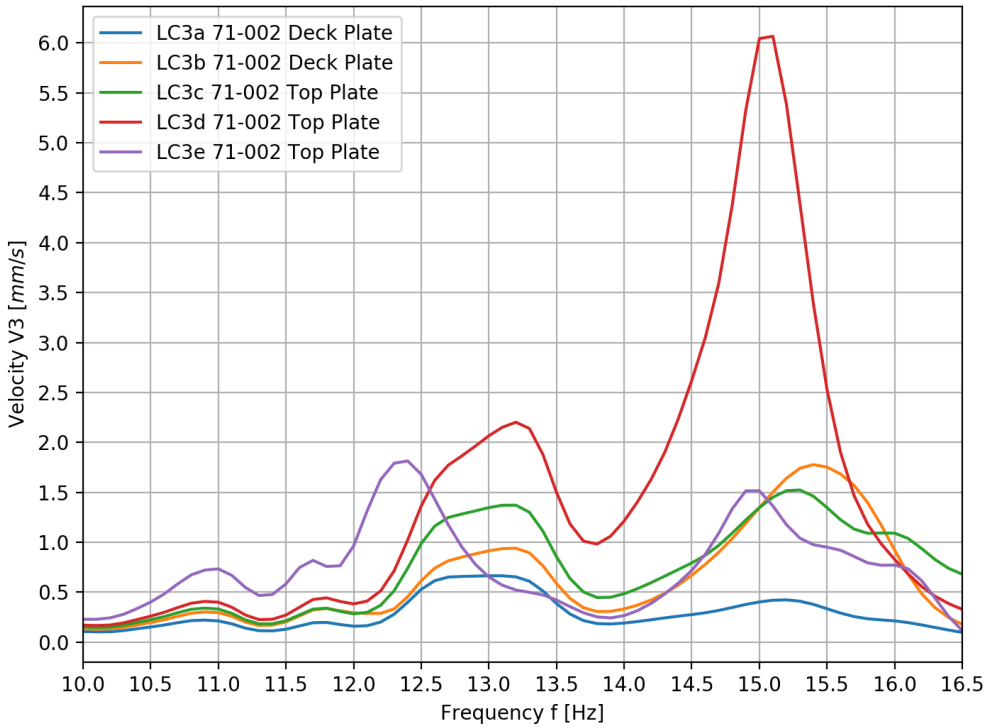

Figure 53. Vertical velocities of the measurement node in cabin 71-002, all load cases.

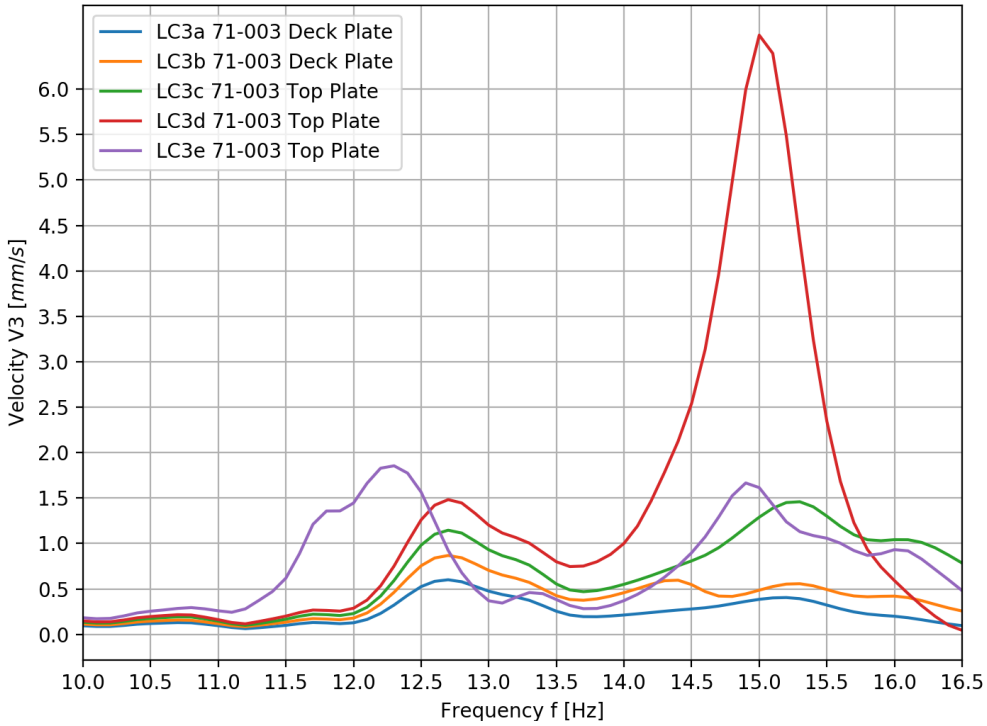

Figure 54. Vertical velocities of the measurement node in cabin 71-003, all load cases.

The vertical velocity results from the measurement node in the cabin 71-019 are presented in Figure 55. In this cabin, a significant peak in vibration levels does not exists when load cases are compared. Thus, it can be deduced that the peaking velocity was due to the local behavior since 71-002 and 71-003 are adjacent cabins i.e. the vibration peak did not occur only because of the floating floor structure.

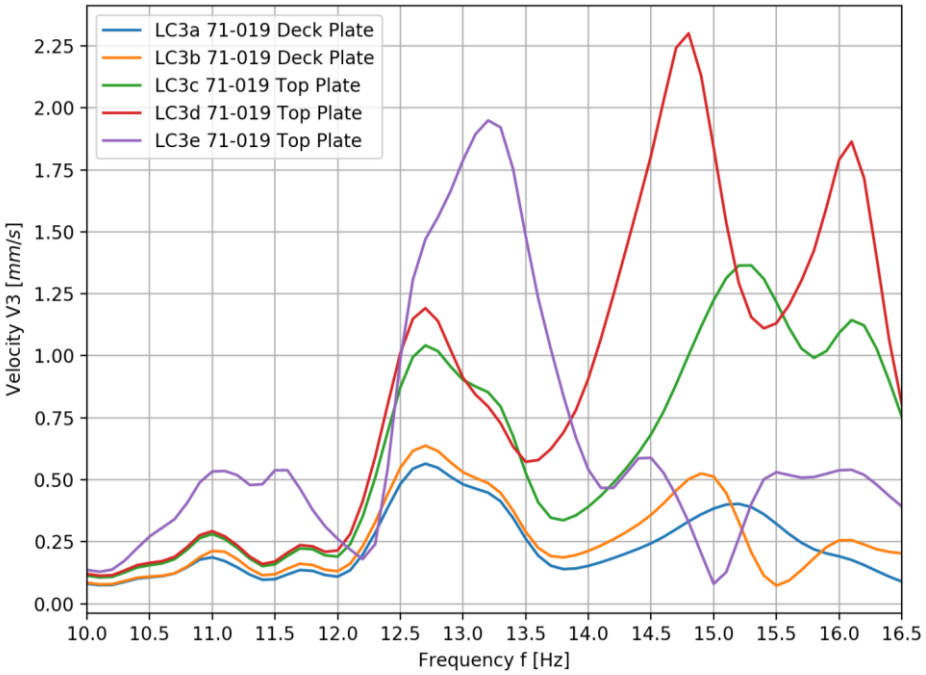

Figure 55. Vertical velocities of the measurement node in cabin 71-019, all load cases.

The vibration levels in all cabins were compared by using each load case. The comparison was done to investigate if cabins with known vibration problems stand out when the vibration levels are compared.

Figure 56 and Figure 57 shows vibration levels of all cabins in the accommodation area without the implemented floating floor structure. Figure 56 represents bare deck situation without additional loading and Figure 57 the situation where cabin loads of 360 kgm^{-2} are applied on the deck plating.

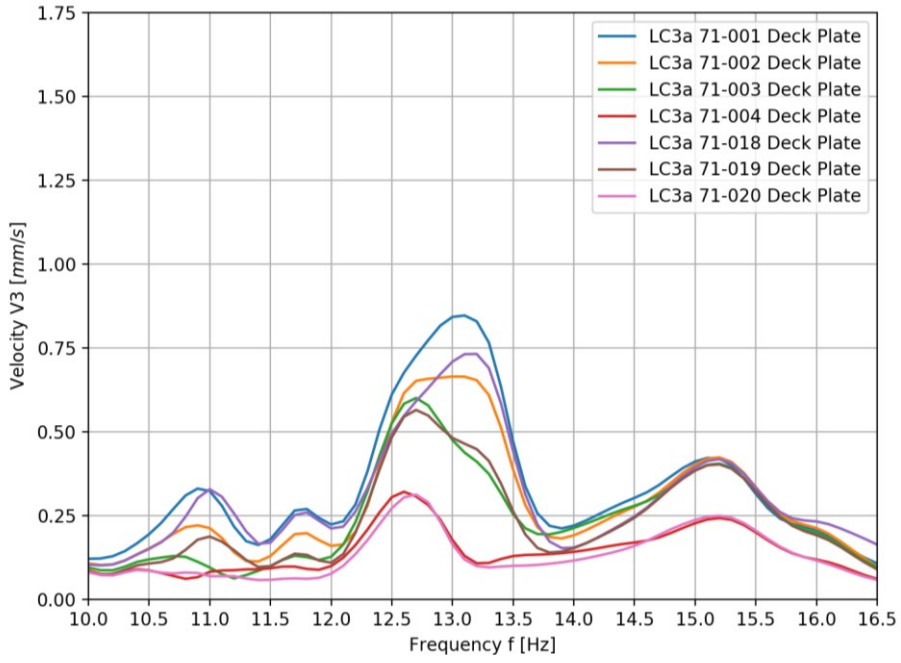

Figure 56. LC3a - Bare Deck, no cabin masses included - Vibration levels of all cabins in the accommodation area.

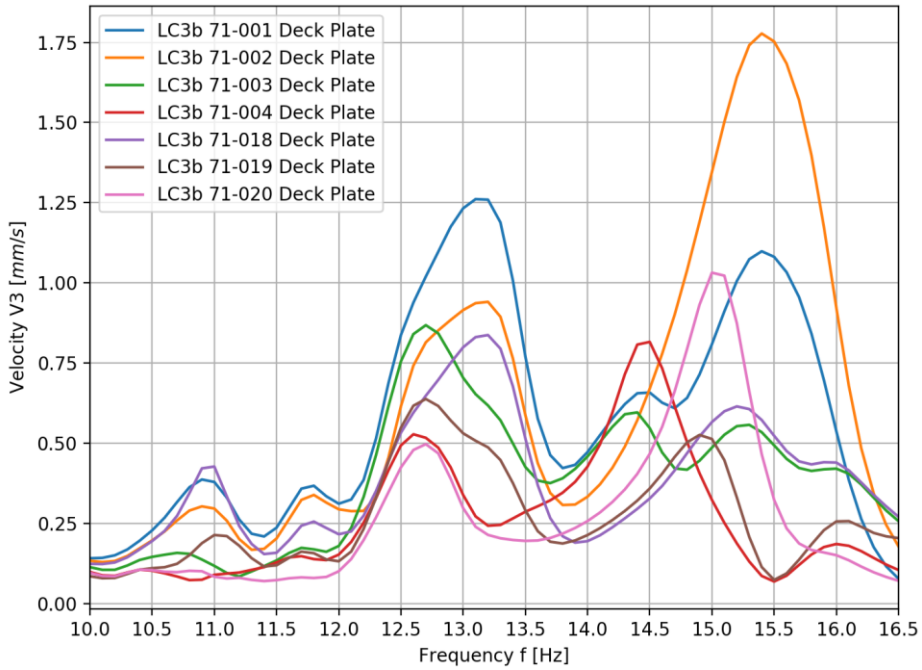

Figure 57. LC3b - Bare Deck with cabin masses included - Vibration levels of all cabins in the accommodation area.

Based on the results presented in Figure 56 and Figure 57, cabins where vibration problems occurred, that is cabins 71-002, 71-003 and 71-019, did not stand out. However, when models with implemented floating floor structures were studied, some auspicious results were discovered. For instance, when the floating floor model LC3c was studied (Figure 58), those cabins had higher vibration levels, especially around 15.25 Hz.

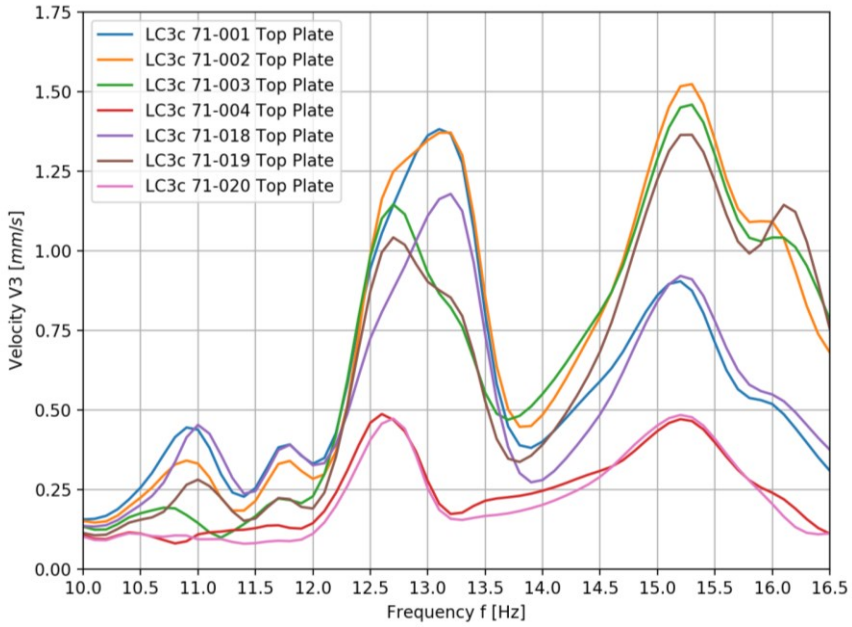

Figure 58. LC3c – Floating Floor without cabin masses - Vibration levels of all cabins in the accommodation area.

As seen already, the load case LC3d generated significant vibration peaks in cabins 71-002 and 71-003. This can be also seen in the following results in Figure 59. However, in this load case the cabin 71-019 did not stand out as clearly as in previous load case.

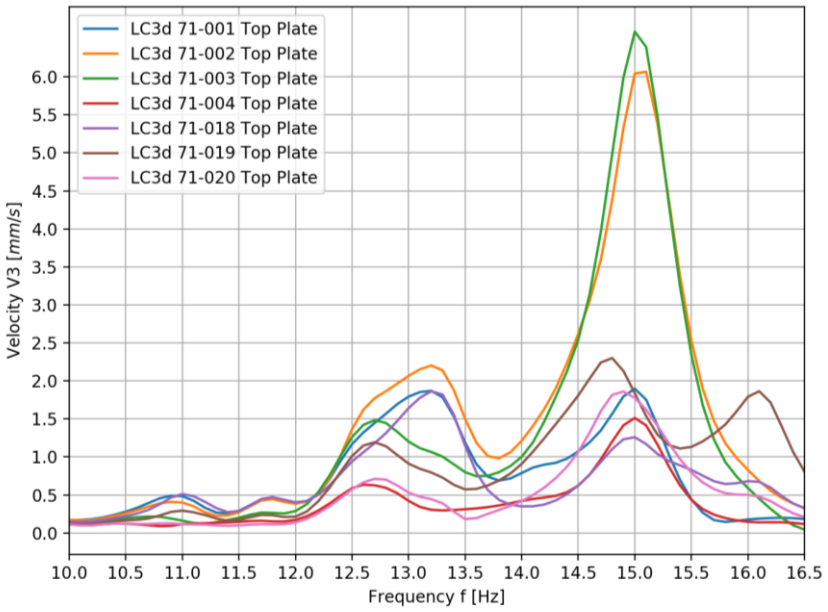

Figure 59. LC3d – Floating Floor with cabin masses of 160 kgm^{-2} - Vibration levels of all cabins in the accommodation area.

When the last load case closest to reality was studied i.e. LC3e, once again quite promising results were obtained. Similarly, as in case of LC3c, cabins 71-002, 71-003 and 71-019 had higher vibration levels than other cabins in the accommodation area.

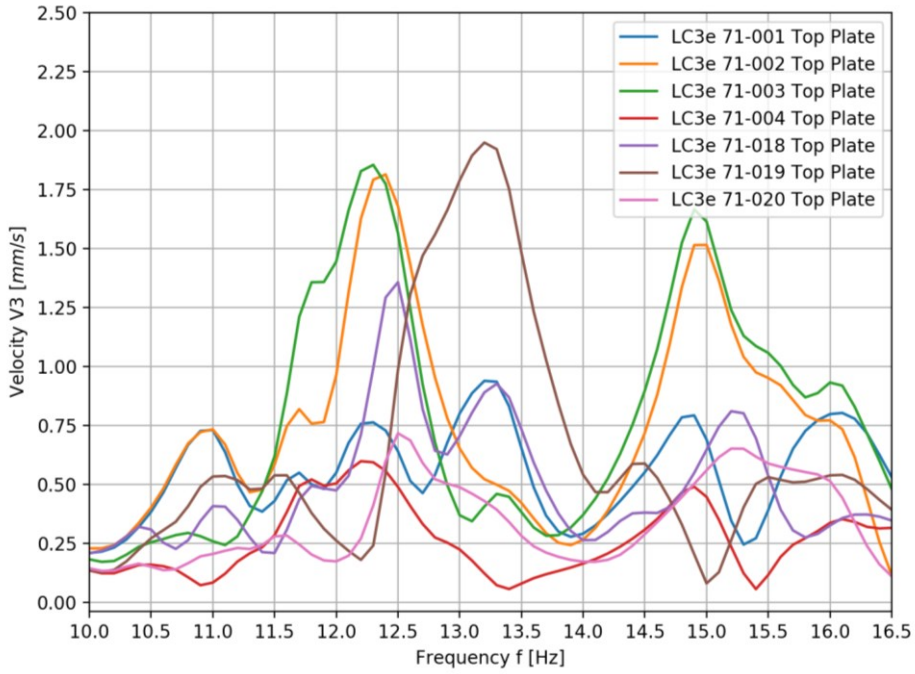

Figure 60. LC3e - Floating Floor with cabin masses of 360 kgm^{-2} - Vibration levels of all cabins in the accommodation area.

Finally, the vibration velocities were compared between deck plating and the top plate. The cabin 71-019 was used as an example and all floating floor load cases were investigated i.e. LC3c, LC3d and LC3e. The results are presented in Figure 61. From these results it can be seen that the modelled floating floor structure amplifies vibration levels through the mineral wool layer that is typical behavior of floating floor structures below the structures natural frequency.

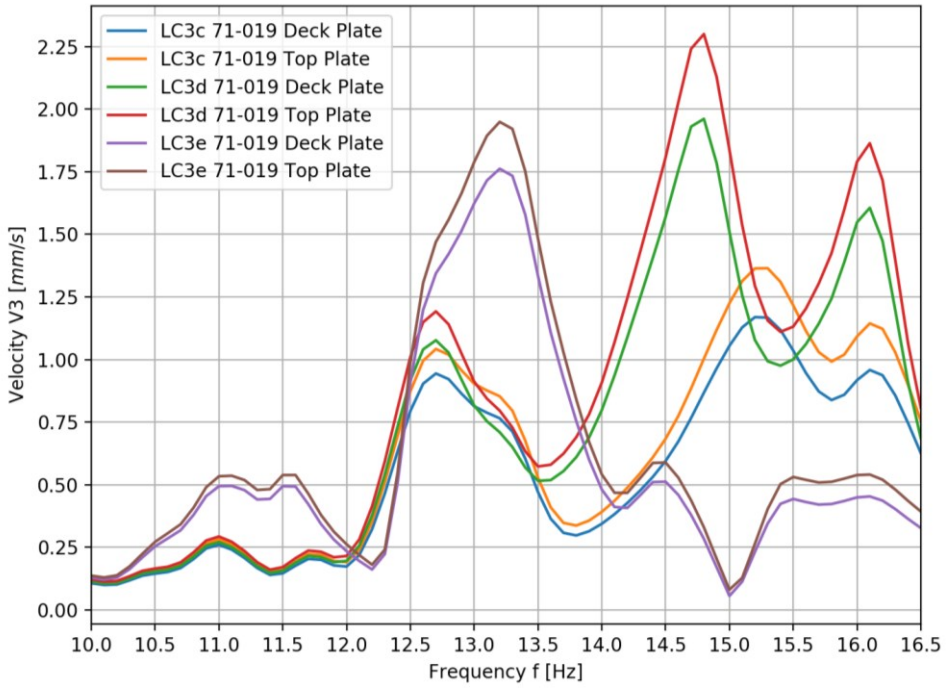

Figure 61. Transmission loss comparison

8.4.3 Interpretation of Results

The vibration analysis of the studied accommodation area at the 2nd Bridge Deck yielded fairly auspicious results. It was known that the cabins 71-002, 71-003 and 71-019 faced significant vibration problems during the seatrials of the ship. The conducted vibration analysis back then did not highlight these cabins as possibly critical locations and neither did vibration analysis in this thesis when only bare deck situations were investigated. However, when this very simplified model of a floating floor was implemented into the Finite Element model of the studied area, these critical locations can be distinguished for having bit higher vibration velocities than other cabins at the area.

This can be already seen when the floating floor model was implemented without cabin masses as seen in the results of LC3c (Figure 58). In this case two different peaks were occurring. The first peak took place at the frequency of 13 Hz where vibration levels at all critical cabins peaked. Also, adjacent cabins at the aft side of critical cabins peaked at that frequency. However, at the next peak around 15 Hz, only the critical cabins stood out and other cabins had smaller vibration levels.

When cabin masses of 160 kgm^{-2} were applied (Figure 59) in LC3d, the cabins 71-002 and 71-003 had a very significant vibration level peak at the frequency of 15 Hz. In this case also the cabin 71-019 had higher vibration levels than other cabins, but the difference was not that significant.

In the load case LC3e, the floating floor with 360 kgm^{-2} cabin masses (Figure 60), once again these critical cabins stood out as higher levels of vibrations. However, this time the frequencies of these vibration peaks were more spread out. The cabins 71-002 and 71-003 peaked at the same frequencies, around 12.25 Hz and 15 Hz, but the cabin 71-019 had its velocity peak only at the frequency of 13.25 Hz.

Based on these analyses and results, it can be said that the developed modelling method for floating floor could produce better results when it comes to locating possible hotspots and critical locations. However, achieving a comprehensive verification of the modelling method, measurements of a real structure would be needed. Since there are no extensive amount of vibration measurement data from the actual ship available, the comparison of vibration levels is not that relevant.

9 Conclusions and Future Studies

In this thesis dynamic behavior of floating floor structures was studied and the design process was enhanced when it comes to vibration analysis of ship structures with implemented floating floor structures. Vibration analysis methods of ship structures were studied in general and these analysis techniques were utilized to take into account floating floor structures.

Different approaches were investigated briefly to find out the most suitable and promising approach. Initially three different approaches were considered, a simple mathematical model based on the basic concepts of vibration dynamics, a modelling method based on the finite element method and an analysis method based on the experimental modal analysis. For further development, the modelling approach based on the finite element method was chosen. From the design process point of view this method was considered the most practical approach since the means of finite element analysis are already used in the design process.

The structure of the floating floor was modelled as a construction of shell and solid elements. The steel deck and top plates were modelled as shell elements and the mineral wool layer between as solid elements. The used material properties for the mineral wool were defined based on the behavior of mineral wool under static loading and declared dynamic stiffness values by the mineral wool manufacturers. The material model was simplified to use only basic isotropic material properties, Young's modulus, Shear modulus and Poisson's ratio. The used material model was validated by comparing the behavior of the FE-model with the results obtained from the definition of dynamic stiffness and with the measurement data received from Sika Group.

The developed submodelling method was based on transferring the response of the global model into the submodel in node to node basis. The functionality of the submodel was validated by comparing the response of the submodel with the response of the global model. Both models yielded similar results, therefore the selected submodelling method was considered to function as desired.

In the case study, the finite element model of the ship NB 511 was utilized. The response of the global model was solved by using the direct frequency response analysis method. The analysis was carried out by using Femap 11 with NX Nastran solver. Excitations from the propulsion system and main engines were applied in FE-analysis. The response obtained from the global analysis was transferred into the submodel of the 2nd Bridge Deck of the ship. The responses of different floor structure configurations were solved from the FE-model. The studies included two bare deck configurations and three different floating floor configurations. All floating floor load cases had the same floating floor construction but different loading.

The interpretation of the analysis results showed that the higher vibration levels can be distinguished at the cabins where excessive vibrations were found during seatrials, when compared with vibration levels of other cabins in the accommodation area. These results seem quite auspicious when the localization of critical areas is considered. Nevertheless, for complete verification of the modelling method, measurements of real structures would be needed.

Finally, a few notions from a future studies point of view. The used model produced promising results when used for the localization of critical areas, however, when it comes to the analysis of the magnitude of vibration levels, further studies are needed. A mockup of a simple floating floor structure could be tested in a laboratory environment. By applying a wide range of excitations on the structure and measuring responses could provide plenty of valuable information about the behavior of floating floor structures. In this thesis, a straightforward modelling method that serves as a design tool was developed, however, there is a need for more thorough studies on the behavior of floating floor structures at the frequencies below 50 Hz where most significant the excitations occur.

References

[1] Arctech Helsinki Shipyard, "Multifunctional Icebreaking Supply Vessels - Vitus Bering and Aleksey Chirikov," [Online]. Available: http://arctech.fi/wp-content/uploads/NB506-507_EN_2013_www.pdf. [Accessed 27 February 2019].

[2] ISO 20283-5, *Mechanical vibration -- Measurement of vibration on ships -- Part 5: Guidelines for measurement, evaluation and reporting of vibration with regard to habitability on passenger and merchant ships,* 2017.

[3] Arctech Helsinki Shipyard, "Icebreaking Offshore Supply Vessel - NB 511 for Sovcomflot," [Online]. Available: http://arctech.fi/fi/wp-content/uploads/NB511_EN_update_web.pdf. [Accessed 27 February 2019].

[4] V. Bertram, Practical Ship Hydrodynamics, Oxford: Elsevier, 2012.

[5] American Bureau of Shipping, "Guidance Notes on Ship Vibration," American Bureau of Shipping, Houston, 2006.

[6] American Bureau of Shipping, "Guidance Notes on Ship Vibration," Spring, 2018.

[7] Lloyd's Register, "Guidance Notes - General Overview of Ship Structural Vibration Problems," 2015.

[8] D. Woodyard, Pounders Marine Diesel Engines and Gas Turbines, Oxford: Elsevier, 2009.

[9] B. Yong and J. Wei-Liang, Marine Structural Design, Oxford: Butterworth-Heinemann , 2015.

[10] I. Asmussen, W. Menzel and H. Mumm, "Ship Vibration," Germanischer Lloyd, Hamburg, 2001.

[11] Siemens Product Lifecycle Management Software, *NX Nastran - Basic Dynamic Analysis User's Guide,* 2016.

[12] S.-I. Cha and H.-H. Chun, "Insertion loss prediction of floating floors used in ship cabins," *Applied Acoustics 69,* pp. 913-917, 2008.

[13] Sika Services AG / Marine, "Sikafloor Marine Systems - Floating Floor and Combination Systems - Presentation," 2018.

[14] Sika Group, "Sikafloor® Marine FLF Type 8.2, Litosilo Steel + sikaForce®-7752 FRW," 21 June 2018. [Online]. Available: https://www.sika.com/en/solutions_products/industry-markets/marine-market/download/sound-test-reports.html. [Accessed 31 March 2019].

[15] O. A. B. Hassan, Building Acoustics and Vibration, Singapore: World Scientific Publishing, 2009.

[16] J. Lalla, *Noise Insulating Floors in Shipbuilding (B.Eng Thesis),* Satakunta University of Applied Sciences, 2012.

[17] Sika Group, "Sikafloor® Marine Visco EM 5 VEM X + 3 mm Steel," 30 October 2018. [Online]. Available: https://www.sika.com/en/solutions_products/industry-markets/marine-market/download/sound-test-reports.html. [Accessed 31 March 2019].

[18] Sika Group, ”Sikafloor® Marine Visco FLF Type 26, VEM X Steel + Litosilo Steel + SikaFrce®-7752 FRW,” 21 June 2018. [Online]. Available: https://www.sika.com/en/solutions_products/industry-markets/marine-market/download/sound-test-reports.html. [Haettu 31 March 2019].

[19] EN 29052-1:1992, *Acoustics - Determination of dynamic stiffness - Part 1: Materials used under floating floors in dwellings,* 1992.

[20] A. Schiavi, "Improvement of impact sound insulation: A constitutive model for floating floors," *Applied Acoustics,* vol. 129, pp. 64-71, 2018.

[21] J.-H. Song, S.-Y. Hong and W.-H. Joo, "Analysis of structure-borne noise in ship cabins using a floating floor with an inserted viscoelastic layer," *Journal of Marine Science and Technology,* vol. 14, pp. 127-135, 2009.

[22] E. Avi, I. Lillemäe, J. Romanoff and A. Niemelä, "Equivalent shell element for ship structural design," *Ships and Offshore Structures,* vol. 10, no. 3, pp. 239-255, 2015.

[23] J. He and Z.-F. Fu, Modal Analysis, Oxford: Butterworth-Heinemann, 2001.

[24] EN 826:2013, *Thermal insulating products for building applications. Determination of compression behaviour,* 2013.

[25] Paroc Group Oy, "Marine and Offshore products and solutions," April 2019. [Online]. Available: https://www.paroc.com/-/media/files/brochures/com/marine-and-offshore-products-and-solutions-paroc-int.ashx?la=en. [Accessed 7 April 2019].

[26] W. S. Vorus, The Principles of Naval Architecture Series Vibration, Jersey City: The Society of Naval Architects and Marine Engineers, 2010.

[27] Sika Group, "Flooring and Acoustic Damping - Sikafloor® Marine," 17 November 2017. [Online]. Available: https://www.sika.com/en/solutions_products/industry-markets/marine-market/download/printed-media.html. [Accessed 30 March 2019].